PB85-169860

Relationship of Fly Ash Composition Refractive Index, and Density to In-Stack Opacity

Atmospheric Research Group, Altadena, CA

Prepared for

Environmental Protection Agency
Research Triangle Park, NC

Feb 85

U.S. Department of Commerce
National Technical Information Service
NTIS

PB85-169860

EPA/600/7-85/003
February 1985

THE RELATIONSHIP OF FLY ASH COMPOSITION, REFRACTIVE INDEX, AND DENSITY TO IN-STACK OPACITY

by

S. J. Cowen
Atmospheric Research Group
Altadena, California 91001

and

D. S. Ensor
Research Triangle Institute
Research Triangle Park, North Carolina

Project Officer: L. E. Sparks

Cooperative Agreement #R806718-01

AIR AND ENERGY ENGINEERING RESEARCH LABORATORY
OFFICE OF RESEARCH AND DEVELOPMENT
U.S. ENVIRONMENTAL PROTECTION AGENCY
RESEARCH TRIANGLE PARK, NC 27711

REPRODUCED BY
NATIONAL TECHNICAL
INFORMATION SERVICE
U.S. DEPARTMENT OF COMMERCE
SPRINGFIELD, VA. 22161

REPRODUCED BY
NATIONAL TECHNICAL
INFORMATION SERVICE
U.S. DEPARTMENT OF COMMERCE
SPRINGFIELD, VA. 22161

TECHNICAL REPORT DATA (Please read Instructions on the reverse before completing)		
1. REPORT NO. EPA/600/7-85/003	2.	3. RECIPIENT'S ACCESSION NO. PB85 169860/AS
4. TITLE AND SUBTITLE The Relationship of Fly Ash Composition, Refractive Index, and Density to In-stack Opacity		5. REPORT DATE February 1985
		6. PERFORMING ORGANIZATION CODE
7. AUTHOR(S) S. J. Cowen (ARG) and D. S. Ensor (RTI)*		8. PERFORMING ORGANIZATION REPORT NO.
9. PERFORMING ORGANIZATION NAME AND ADDRESS Atmospheric Research Group Altadena, California 91001		10. PROGRAM ELEMENT NO.
		11. CONTRACT/GRANT NO. R806718-01
12. SPONSORING AGENCY NAME AND ADDRESS EPA, Office of Research and Development Industrial Environmental Research Laboratory Research Triangle Park, NC 27711		13. TYPE OF REPORT AND PERIOD COVERED Grant Final; 6/81 to 5/82
		14. SPONSORING AGENCY CODE EPA/600/13

15. SUPPLEMENTARY NOTES IERL-RTP project officer is Leslie E. Sparks, MD-61, 919/541-2925. (*) Research Triangle Institute, Research Triangle Park, NC 27709.

16. ABSTRACT The report gives results of an investigation of the refractive index, density, and composition of fly ash from coal-fired boilers, aimed at determining: (1) the interrelationship of refractive index and composition, and (2) the significance of ash properties on in-stack plume opacity. A survey was made of 14 ash samples representing a wide range of coals. Light absorption was measured using the Integrating Plate Method, which compares light absorption through a clean filter to that through a filter with a single layer of aerosol. Only absorption is measured, while scattered light is integrated equally for both cases. This technique requires fine particles (volume absorbers) for easy interpretation of results. The technique was calibrated using an aerosol, methylene blue, with known absorption characteristics. The real part of the refractive index was measured by an oil immersion technique. The real refractive index and density were found to be highly correlated with composition with a multilinear regression equation. The absorbing refractive index was well correlated with ash carbon content. The modeling of in-stack opacity showed a weak dependence on ash optical properties for the range of ashes studied. The effect of the real part of the refractive index on opacity tends to be counterbalanced by particle density effects. Furthermore, most fly ash absorbs relatively little light.

17. KEY WORDS AND DOCUMENT ANALYSIS

a. DESCRIPTORS		b. IDENTIFIERS/OPEN ENDED TERMS	c. COSATI Field/Group	
Pollution	Coal	Pollution Control	13B	21D
Fly Ash	Boilers	Stationary Sources	21B	13A
Opacity			14G	
Refractivity			20F	
Density				
Composition				

18. DISTRIBUTION STATEMENT	19. SECURITY CLASS (This Report)	21. NO. OF PAGES
Release to Public	Unclassified	65
	20. SECURITY CLASS (This page) Unclassified	22. PRICE

EPA Form 2220-1 (9-73)

NOTICE

This document has been reviewed in accordance with U.S. Environmental Protection Agency policy and approved for publication. Mention of trade names or commercial products does not constitute endorsement or recommendation for use.

ABSTRACT

The refractive index, density, and composition of fly ash from coal-fired boilers was investigated. The goals were to determine the inter-relationship of refractive index and composition and to determine the significance of ash properties on in-stack plume opacity. A survey was made of 14 ash samples representing a wide range of coals. Light absorption was measured using the Integrating Plate Method. The Integrating Plate Method compares light absorption through a clean filter to light absorption through a filter with a single layer of aerosol. Only absorption is measured while scattered light is integrated equally for both cases. This technique requires fine particles (volume absorbers) for easy interpretation of results. The technique was calibrated using an aerosol, methylene blue, with known absorption characteristics. The real part of the refractive index was measured by an oil immersion technique. The real refractive index and density were found to be highly correlated with composition with a multilinear regression equation. The absorbing refractive index was well correlated with ash carbon content.

The modeling of in-stack opacity showed a weak dependence on ash optical properties for the range of ashes studied. The effect of the real part of the refractive index on opacity tends to be counterbalanced by particle density effects. Furthermore, fly ash absorbs relatively little light except for very high carbon ashes.

CONTENTS

Section		Page
Abstract		iii
Figures		v
Tables		vi
List of Symbols		vii
Acknowledgments		viii
1.	Introduction	1
2.	Conclusions and Recommendations	3
	Optical properties of fly ash	3
	Integrating plate method	3
	Soot light absorption	3
	Recommendations	4
3.	Experimental Design	5
	Imaginary refractive index	5
	Real refractive index	10
	Carbon analysis	11
	Particle density analysis	11
	Chemical analysis	11
4.	Reduction of Light Absorption Data	13
5.	Results	17
	Calibration	17
	Fly ash light properties	21
	Significance of the material physical properties on in-stack opacity	32
References		37
Appendix A.	Calibration aerosol data	39

FIGURES

Number		Page
1	Schematic diagram of the optical system incorporating the Integrating Plate Method	7
2	Transmission electron microphotograph of a single fly ash particle	9
3	Schematic diagram of helium pycnometer	12
4	Specific absorption coefficient of methylene blue in ammonium sulfate	18
5	Effect of particle density on the real refractive index	23
6	Specific absorption coefficient of fly ash as a function of carbon content	27
7	Microphotograph of soot aerosol (4000X)	29
8	Aerosol size distribution of soot particles	30
9	Imaginary refractive index of fly ash as a function of carbon content	31
10	The effect of the extremes of refractive index and density on the mass extinction coefficient for monodisperse particles	33

TABLES

Number		Page
1	Comparison of the Absorption Measurement Between the Integrating Plate Method and Integrating Sphere	20
2	Summary of Ash Composition (%) and Physical Properties . . .	22
3	Multilinear Regression Analysis of Specific Refractivity and Ash Composition	25
4	Computed Effects of Absorbing Refractive Index on Plume Opacity	35
5	Effect of Submicrometer Soot on Opacity	36

LIST OF SYMBOLS

ENGLISH SYMBOLS

A -- Exposed filter area, cm^2

b_{abs} -- Absorption coefficient (m^{-1})

b_{ext} -- Extinction coefficient (m^{-1})

b_{scat} -- Scattering coefficient (m^{-1})

I -- Transmitted light intensity (lumens)

I_o -- Incident light intensity (lumens)

I' -- Intensity of light through an opal glass and filter with deposited aerosol (lumens)

I_o' -- Intensity of light through an opal glass and blank filter (lumens)

k -- Wave number (μm^{-1})

L -- Illumination pathlength (m)

M -- Particle mass concentration (g/m^3)

M_g -- Particle mass on filter, g

n' -- Real part of the index of refraction

n'' -- Imaginary part of the index of refraction

S_a -- Mass absorption coefficient (m^2/g)

S_m -- Mass extinction coefficient (m^2/g)

S_{va} -- Specific absorption coefficient (m^2/cm^3)

S_{ve} -- Specific extinction coefficient (m^2/cm^3)

GREEK SYMBOLS

λ -- Wavelength of incident light (μm)

ρ -- Particle density (g/cm^3)

ACKNOWLEDGMENTS

We are particularly grateful to Ed Hindman of Colorado State University and Herman Gerber of the U.S. Naval Weapons Laboratory, Washington, DC, for inviting us to participate in the First International Workshop on the Absorption of Light by Aerosols, held at Colorado State University, July 1980. We appreciate the efforts of Jim Gillespie of the U.S. Army Atmospheric Sciences Laboratory, White Sands Missile Range, NM, in analyzing some of our fly ash samples using his integrating sphere technique. We also extend our thanks to Roy Bickelhaupt of Southern Research Institute, Birmingham, AL, for providing the ash samples with chemical analysis. This study was supported by cooperative agreement #R806718-01 with the Environmental Protection Agency, Research Triangle Park, NC.

SECTION 1

INTRODUCTION

Opacity limitations of air pollution emissions are an important aspect of stationary source regulations. However, the engineering approaches needed to design control equipment to meet opacity limits are still under development. Ensor (1972) established the relationship of plume opacity to mass concentration as a function of log-normal particle size distributions of the emission for ideal conditions. More recently, it was determined that the particle size distributions downstream of emission control equipment are usually not log-normal. As a result, development of calculator programs to allow prediction of expected plume opacity from particle size distribution data and mass concentration was the topic of a study by Cowen, Ensor, and Sparks (1980). However, the secondary variables affecting plume opacity such as particle density and refractive index have not been systematically measured under conditions useful for plume opacity prediction. The usual practice has been to assume nominal values of refractive index and particle density.

The present research has two objectives: (1) to measure refractive index and particle density with supporting chemical composition for a wide selection of ashes from utility boilers firing bituminous coal, and (2) to compute the sensitivity of plume opacity to the variation of particle refractive index and density using these data. The survey nature of this study allowed the use of bulk samples taken from ash hoppers at utility plants.

In no previous investigations have all the physical properties required for plume opacity prediction been measured on the same sample of fly ash. Examples of typical fly ash characterization research include determination of the chemical composition of ashes from the major coal fields in the United States by the Bureau of Mines (Gluskoter et al., 1977) and measure-

ments of composition and particle density in size-segregated samples for a single sample of fly ash by Fisher et al. (1978). It should be noted that the refractive index of a material is a complex number. The real part describes the bending of light and the imaginary part describes the absorption of light with subsequent conversion to heat in the material. Two totally different measurements are required to determine this physical property. The measurement of real refractive index is a fairly common practice for mineral and small particle identification (McCrone et al., 1967). Limited measurements of absorptive refractive index have been reported for fly ash: Volz (1973) measured absorption of fly ash in the infrared wavelengths and Nolan (1977) reported the visible light absorption of ash sampled at a university heating plant boiler under limited conditions. Thus, an important contribution of the present research is that a battery of previously developed analytical methods was conducted on a fairly wide range of ash samples. Many of the ash samples were also used by Bickelhaupt (1979) to develop mathematical relationships between electrical resistivity and chemical composition.

Section 2 presents the conclusions and recommendations from the study, the experimental techniques and data reduction are described in Sections 3 and 4, Section 5 contains the reduced data and sensitivity analyses, and Appendix A archives the particle size distribution data from laboratory-generated aerosols used to calibrate the Integrating Plate Method for light absorption measurement.

SECTION 2

CONCLUSIONS AND RECOMMENDATIONS

A survey of the refractive index, density, and composition of 14 different fly ash samples indicates significant interrelationships between their physical and chemical properties. A regression equation was developed with the specific refractivity $[(n'-1)/\rho]$ as a function of the major chemical components of the ash. The regression explains 82 percent of the variability of the data. The imaginary refractive index was found to be correlated to carbon content of the ash, which explains 80 percent of the variability of the data. The imaginary refractive experiments were limited by the accuracy and sample restrictions of the Integrating Plate Method. However, modeling of opacity with typical fly ash size distributions and the ranges of refractive indices indicates that the absorbing refractive index is insignificant. Although pure soot is an effective material for attenuating light, it is usually not of sufficient quantity in boiler emissions to alter the particle size distribution for maximum effect on plume opacity. Opacity was more sensitive to particle density than real refractive index for computations using the extremes of each.

The Integrating Plate Method is semiquantitative and provides results with sufficient accuracy to fulfill the objectives of this study. However, the technique suffers from several sources of error; e.g., an apparent absorption of known transparent materials from scattered light, and alteration of the reflection of the filter surface by the aerosol sample. Because the method is restricted to submicrometer particles, the ash samples required size segregation. Thus, the chemical composition of the total sample may not be representative of the samples used for the absorption measurement. This problem may be responsible for the scatter observed in the imaginary index carbon correlations. The errors in the method were minimized, however, by the use of an empirical correlation developed with a laboratory aerosol.

It is recommended that work be continued to refine the relationship of fly ash specific refractivity to chemical composition. The data base should be expanded to include a wider range of coal ranks and types such as lignite and anthracite. The results of this effort could lend support to studies correlating mass emissions to plume opacity.

At present, additional work is not justified on the aerosol-absorbing refractive index because the relatively large size of fly ash tends to minimize its effects. However, absorption studies may be worthwhile for sources with submicrometer emissions. Identification of these processes would be a useful application of the techniques developed in this study.

SECTION 3

EXPERIMENTAL DESIGN

Bulk fly ash samples from the combustion of a wide range of bituminous coals were collected from a number of sources. Care was taken to include samples from the major coal basins: Appalachian eastern, Illinois mid-western, and western. The samples obtained from Meteorology Research, Inc., and the Southern Research Institute were collected as part of other research projects. The ash was removed from the hoppers of either electrostatic precipitators or baghouses under typical operating conditions and stored in hard plastic containers until needed. Since the objective of the study was to survey the range of physical and chemical properties likely to be associated with the variability of coal, representativeness of the sample of a specific operation condition was not of major interest. Bulk hopper samples were a cost-effective means of obtaining sufficient data on which to base a definition of the importance of refractive index and particle density. The desirability of performing field tests to obtain optimum samples was offset by the need to obtain preliminary data to aid problem definition.

The 14 fly ash samples were split and subjected to a battery of tests. Tests included measurement of the imaginary refractive index and real refractive index, total carbon analysis, particle density analysis, and chemical analysis. The carbon analysis was essential because of the potential relationship of soot concentration to the imaginary refractive index.

IMAGINARY REFRACTIVE INDEX

The method employed to measure imaginary refractive index was nonconventional and therefore requires detailed explanation. No existing aerosol absorption technique is very accurate because of the errors introduced by particle light scattering and the need to work with small samples. One class of techniques involves measuring all the light entering and leaving a

sample of particles and deducing the absorption by difference. This is the basis of the Integrating Sphere and Integrating Plate Methods. Another approach uses the photoacoustic effect, which relates absorption to the sound generated by the heating of a particle passing through a laser beam.

The Integrating Plate Method was selected because of its simplicity and adaptability to source testing methods. The technique was developed by Lin, Baker, and Charlson (1973) who estimated accuracy to be a factor of 2. Later, Weiss et al. (1978) calibrated the instrument with laboratory aerosol and reported an error of ±20 percent. Because of the newness of the method, the calibration was repeated using methylene blue as an absorbing aerosol mixed with ammonium sulfate aerosol as a transparent diluent. (Other potential methods were even less well developed.)

The Integrating Plate Method is a simple direct measurement of aerosol light absorption based on comparison of the transparency of a clean Nuclepore filter with one containing a single layer of particles. The experimental arrangement in the Integrating Plate Method was identical to that reported by Lin, Baker, and Charlson (1973), it being the only description of the device in the literature at that time. Recently, Clarke (1982) described an arrangement in which the sample filter and the opal glass were interchanged.

A Hitachi Model 60 double-beam spectrophotometer with a specially designed double filter holder was used for the comparison. Opal glass behind each filter integrated the transmitted light so that only absorption was recorded. Back scattering probably can be ignored because the reflectivity of the filter is unchanged by the fly ash particle; i.e., the real refractive indices of particles and filters are similar. The double beam automatically gives the ratio of the aerosol absorption to the blank filter. The optical arrangement for a single beam measuring the sample is shown in Figure 1. Nuclepore membrane filters were used because the particles are on the surface of the filter and not embedded as they would be in a fiberglass filter.

The step-by-step procedure for the Integrating Plate Method is:

1. Measure the percent transmittance (I_o') of a blank Nuclepore filter using the spectrophotometer.

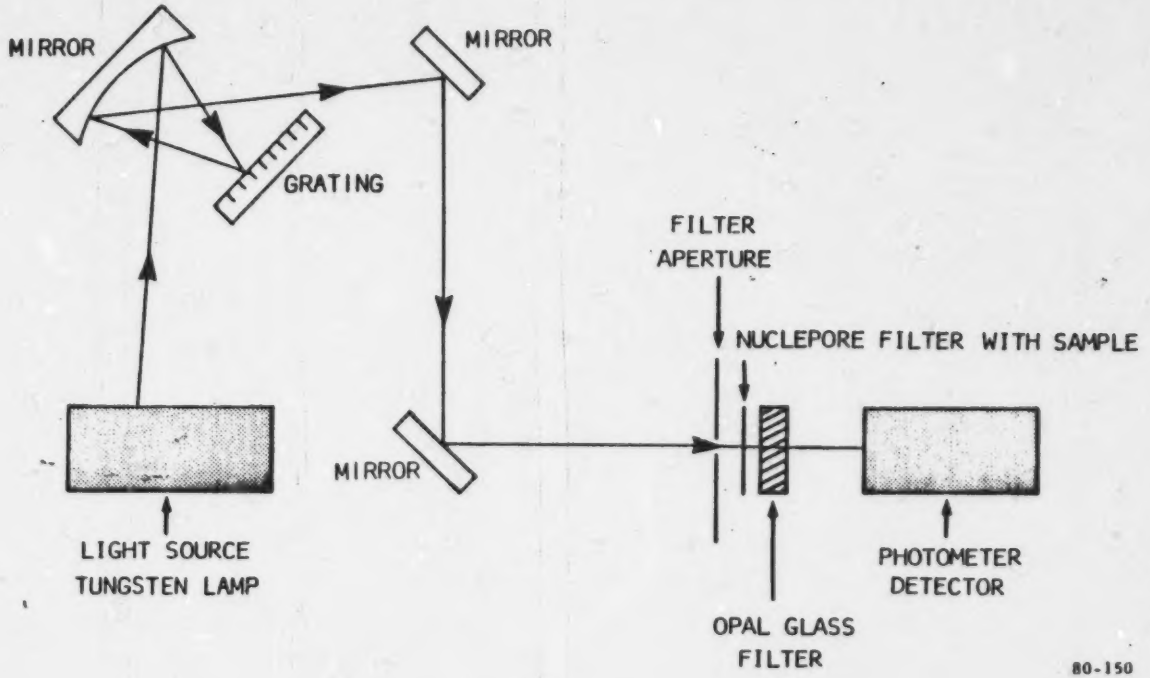

Figure 1. Schematic diagram of the optical system incorporating the Integrating Plate Method.

2. Weigh this filter using an analytical balance with microgram sensitivity.

3. Deposit the submicrometer size aerosol on the filter.

4. Weigh the filter again to determine the aerosol mass loading.

5. Measure the percent transmittance (I') of the filter with aerosol using the spectrophotometer.

The ratio (I'/I_0') is used to calculate the specific absorption coefficient. This calculation is described in Section 4, Reduction of Light Absorption Data.

Bulk ash samples obtained from electrostatic precipitator or baghouse hoppers were suspended in a chamber and only the submicrometer ash particles were collected on the filter for the absorption measurement. A sandblast gun was used as a simple technique for deagglomerating the fly ash by producing a high pressure aerosol stream. A single layer of submicrometer aerosol is required to evaluate the light absorption effects easily. The absorption for submicrometer size aerosols is simply proportional to the aerosol volume according to the Mie theory as decribed by Weiss et al. (1978). The resuspended fly ash was first drawn through a multistage inertial cascade impactor to remove large particles and then through a Model 3071 Thermo Systems, Inc., Electrostatic Classifier to obtain an aerosol with a narrow size distribution and mean diameter of approximately 0.8 μm as shown in Figure 2. The quantity of material collected on each 47-mm filter was approximately 30 to 50 μg as measured by a Cahn 25 balance. A dry gas meter downstream of the filter measured gas volume passing through the filter. The gas volume was used with the filter area to compute an effective optical pathlength and the volume absorption coefficient.

The single layer of ash on the filter is required to avoid multiple scattering effects that would bias the absorption measurement. The most difficult part of this measurement is obtaining enough submicrometer material without large particle contamination. The accuracy of the experiments depends on the quality of this separation and the sensitivity of the analytical balance. A balance with microgram accuracy is highly desirable for an accurate absorption measurement.

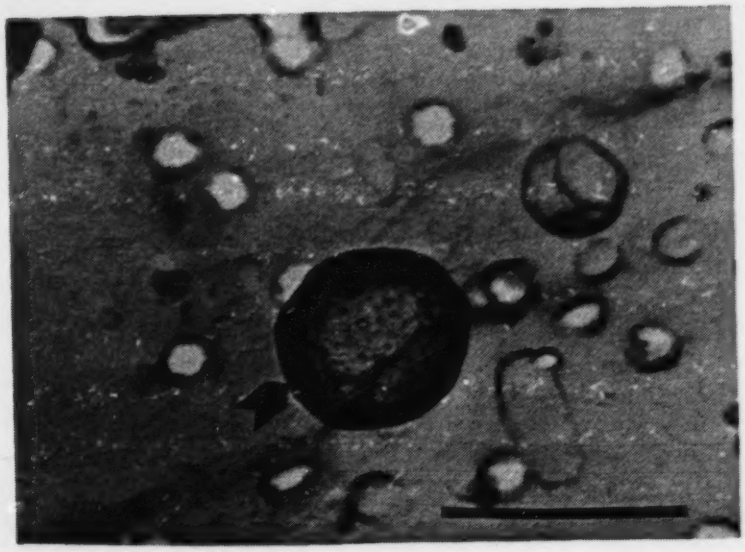

81-170

Figure 2. Transmission electron microphotograph of a single fly ash particle. The line is approximately 1 μm in length.

An experimental problem in determining absorption vs. graphitic carbon content is the inhomogeneity of the hopper ash samples. The hopper samples often contain black particles with radii greater than 10 μm that will not be analyzed in the absorption experiment yet will increase the measured carbon content of the ash sample unless they are removed before the carbon analysis. Thus, correlations between carbon content and absorption will be erroneous if the heterogeneity is not examined and the large particles, thought to be char, are not removed.

Although the Integrating Plate Method is simple to apply, the relatively small quantity of absorption, compared to light scattering, makes it intrinsically difficult to measure accurately.

REAL REFRACTIVE INDEX

The real part of the refractive index was measured by comparing the refractive index of the particle with that of standard immersion oils. The technique is described in detail by McCrone et al. (1967). A small quantity of the fly ash sample was spread onto a glass slide allowing identification of individual particles with an optical microscope. A drop of immersion oil, the refractive index of which was known to four significant figures, was placed on a single particle. The Becke line is the boundary observed between a particle and the fluid in which it is placed if their refractive indexes differ. By moving the microscope in and out of focus and observing the apparent movement of the Becke line, the analyst was able to determine if the fluid had a greater or lesser refractive index than the particle. The refractive index of the particle was determined by repeating the procedure until the refractive index of the oil matched the particle.

The measurement of fly ash refractive index also is affected by the heterogeneity of the ash particles. Certain particles may have a higher refractive index than other particles. A qualitative judgment was made so that an "effective" refractive value represented at least 80 percent of the observed particles.

CARBON ANALYSIS

West Paine Laboratories, Baton Rouge, LA, performed a carbon analysis of the ash samples by standard methods. Approximately 1.0 g of ash was accurately weighed and placed in a tube furnace. The furnace was heated to 800° C until the samples were completely ashed. The CO_2 given off was trapped in a CO_2-free NaOH solution and then was measured by a Beckman Total Organic Carbon Analyzer.

PARTICLE DENSITY ANALYSIS

The fly ash particle density was measured using a Micromeritics Helium Pycnometer. This instrument measures the volume change associated with the change in pressure of a nonabsorbing gas such as helium. A schematic diagram of the instrument is shown in Figure 3. The volume of the sample is measured by comparison to a standard stainless steel ball bearing of known volume.

CHEMICAL ANALYSIS

The ash mineral analysis was performed using spark source mass spectroscopy by Pacific Spectral Laboratory, Los Angeles, CA. This analysis provided the following major mineral components: lithium, sodium, magnesium, calcium, iron, aluminum, silica, titanium, potassium, phosphorous, and sulfur.

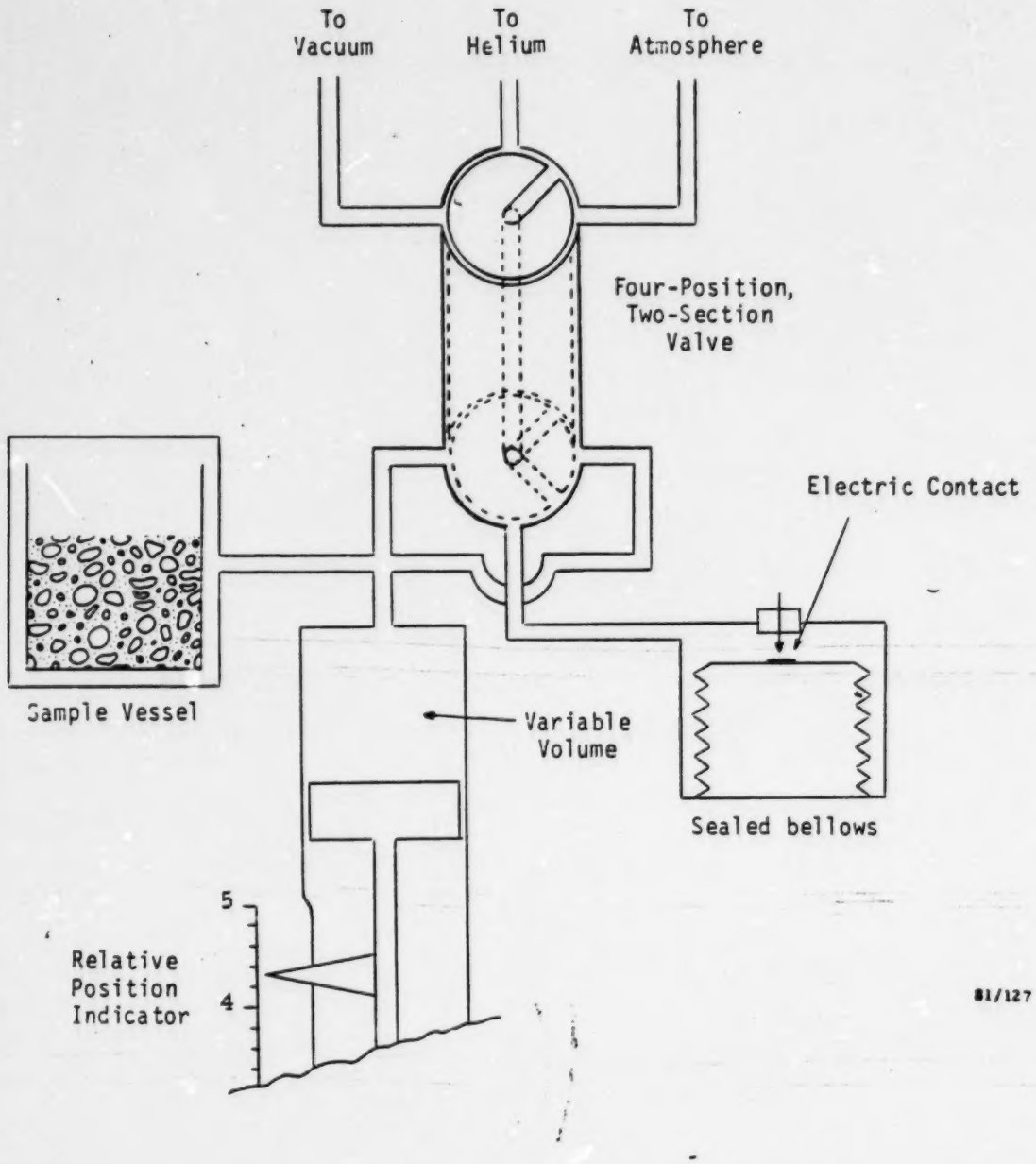

Figure 3. Schematic diagram of helium pycnometer.

SECTION 4

REDUCTION OF LIGHT ABSORPTION DATA

This study represents an extension of the work of Lin, Baker, and Charlson (1973) and Weiss (1980). Previous investigators measured atmospheric aerosols, which typically have a moderately absorbing imaginary refractive index in the range of 0.01. Source aerosols could have a wide range of refractive indices from 10^{-4} to 0.6, depending on soot concentration. And if field testing were conducted as a follow-on, a wide range of concentrations would be experienced. Because of the novel application of the technique and the problems encountered in this study, an extensive calibration program was conducted. The program consisted of development of a calibration curve using methylene blue as an absorbing material with mixtures of ammonium sulfate, participation in the First International Workshop on Light Absorption by Aerosols, and an exchange of samples with another laboratory.

One error in the technique introduced by the alteration of the surface reflections from the sample in the filter was recently discussed by Clarke (1982). Another source of error not quantified at this time results from light scattered from the aerosol particles but not captured by the detector. This error depends on the concentration and absorption of the aerosol and becomes important for materials with small imaginary refractive indices.

The absorption per unit volume of fly ash from the Integrating Plate Method is determined by applying the Beer-Lambert Law to the spectrophotometric readings. Although a double-beam instrument was used, it was operated in a single-beam mode because the beams were not sufficiently powerful to penetrate two opal glasses and two Nuclepore filters and still record 100 percent transmittance readings. Under the single-beam operation, the filter deposited with aerosol was ratioed to the blank filter using the identical blank reference filter in the second beam.

The transmission of light through a volume containing an aerosol is described by the Beer-Lambert Law:

$$\text{Light transmittance} = I/I_0 = \exp(-b_{ext}L) \qquad (1)$$

where

I = is the transmitted light

I_0 = the incident light

b_{ext} = the light extinction coefficient

L = the illumination pathlength.

The light extinction coefficient is the sum of the scattering coefficient (b_{scat}) and the absorption coefficient (b_{abs}).

The ratio of intensity (I') of light transmitted through the opal glass and a filter deposited with aerosol to the intensity (I_0') transmitted through an opal glass and blank filter can be used to calculate the absorption coefficient:

$$I'/I_0' = \exp(-b_{abs}L) \; . \qquad (2)$$

A mass absorption coefficient is defined by the following equation:

$$I'/I_0' = \exp - (S_a \, M \, L) \; . \qquad (2a)$$

The relationship of the particle mass concentration M and optical pathlength is given by:

$$M \, L = M_g/A \qquad (2b)$$

where

M_g = the particle mass on the filter

A = the exposed filter area.

The mass absorption coefficient is a useful bulk property. However, when mixtures of materials with dissimilar densities are used, it is better to use a specific volume absorption coefficient (ratio of the absorption coefficient to the aerosol volume concentration) to allow correction for particle density.

$$S_{va} = S_a \, \rho \qquad (3)$$

The data reduction equation is given by:

$$I/I_o = \exp\ (-S_{va}\ M_g/\rho\ A)\ . \qquad (4)$$

This equation allows computation of S_{va} from measured I/I_o, M_g, ρ, and A.

The remaining data reduction step is to convert S_{va} to the imaginary refractive index of the material n". Two approaches were considered: a relationship developed from the Raleigh light scattering theory and direct calibration. Both approaches rely on the proportion of the absorption of light to the volume of the aerosol particles.

This equation reduction using the Raleigh theory was developed by Weiss (1980):

$$n'' = S_{va}\ (n'^2 + 2)^2/18\ k\ n' \qquad (5)$$

where

$k = 2\ \pi/\lambda$ (λ = the wavelength of light)

n' = the real refractive index.

The assumptions used to develop this equation are that the particles must be smaller than the wavelength of light (<0.5 μm), the imaginary refractive index should be much smaller than the real imaginary refractive index, and the particles on the surface should scatter in a manner similar to suspended particles.

The second approach was based on calibrating the instrument with a laboratory aerosol of particle shape and size similar to fly ash with known absorption characteristics. This was accomplished with an aerosol of spherical ammonium sulfate particles containing various amounts of methylene blue dye to obtain various degrees of light absorption. The calibration S_{va} is then proportional to the product of the n" of methylene blue and its weight percent in the ammonium sulfate aerosol, a nonabsorbing material. The n" of the ash sample is calculated in the following manner. The S_{va} of the ash sample is plotted on the methylene blue ammonium sulfate calibration curve. The fraction of methylene blue corresponding to this plotted point multiplied by the n" of methylene blue (in this case, 0.1) equals the n" of the ash sample. For example, an ash sample with an S_{va} equal to 2 m^2/cm^3 corresponds approximately to 10 percent methylene blue in ammonium sulfate

when plotted on the calibration curve. The imaginary refractive index is then 10 percent of 0.1 or 0.01. The real part of the refractive index does not strongly affect the absorption measurement because the fly ash and filter have similar real refractive indices.

For the present study, the calibration aerosol was the preferred approach because it was believed to be more accurate than the Weiss equation for small imaginary refractive indices. However, because pure methylene blue has a smaller imaginary refractive index than pure soot (0.1 versus 0.66), the direct calibration may yield low imaginary refractive indices for highly absorptive samples.

SECTION 5

RESULTS

This section discusses both the laboratory work and mathematical modeling used to determine the significance of the findings with respect to expected in-stack plume opacity. The calibration consisted of extensive measurements with laboratory aerosol, participation in a workshop, and the exchange of samples with another laboratory. The fly ash physical property and chemical composition are reported with correlations between significant variables. The modeling effort addressed the following issues: the range of opacity expected with the measured range of particle refractive index and density, the effect of imaginary refractive index (or soot) under typical conditions, and the effect of soot on opacity under atypical conditions.

CALIBRATION

Methylene Blue--Ammonium Sulfate Aerosol

The fly ash absorption measurements were calibrated using methylene blue aerosol with known absorption characteristics. Different levels of aerosol absorption were made by nebulizing solutions of ammonium sulfate, a nonabsorbing aerosol, with different concentrations of methylene blue. Figure 4 shows the calibration curve with the specific absorption coefficient versus percent methylene blue in ammonium sulfate aerosol. These aerosols were generated at the First International Workshop on Light Absorption by Aerosols at the Colorado State University Cloud Simulation and Aerosol Laboratory and MRI's aerosol laboratory. The details of the workshop are given by Hindman, Horn, and Finnegan (1982).

The calibration curve for low absorbing aerosols (methylene blue content less than 3 percent) is offset from zero by the presence of an

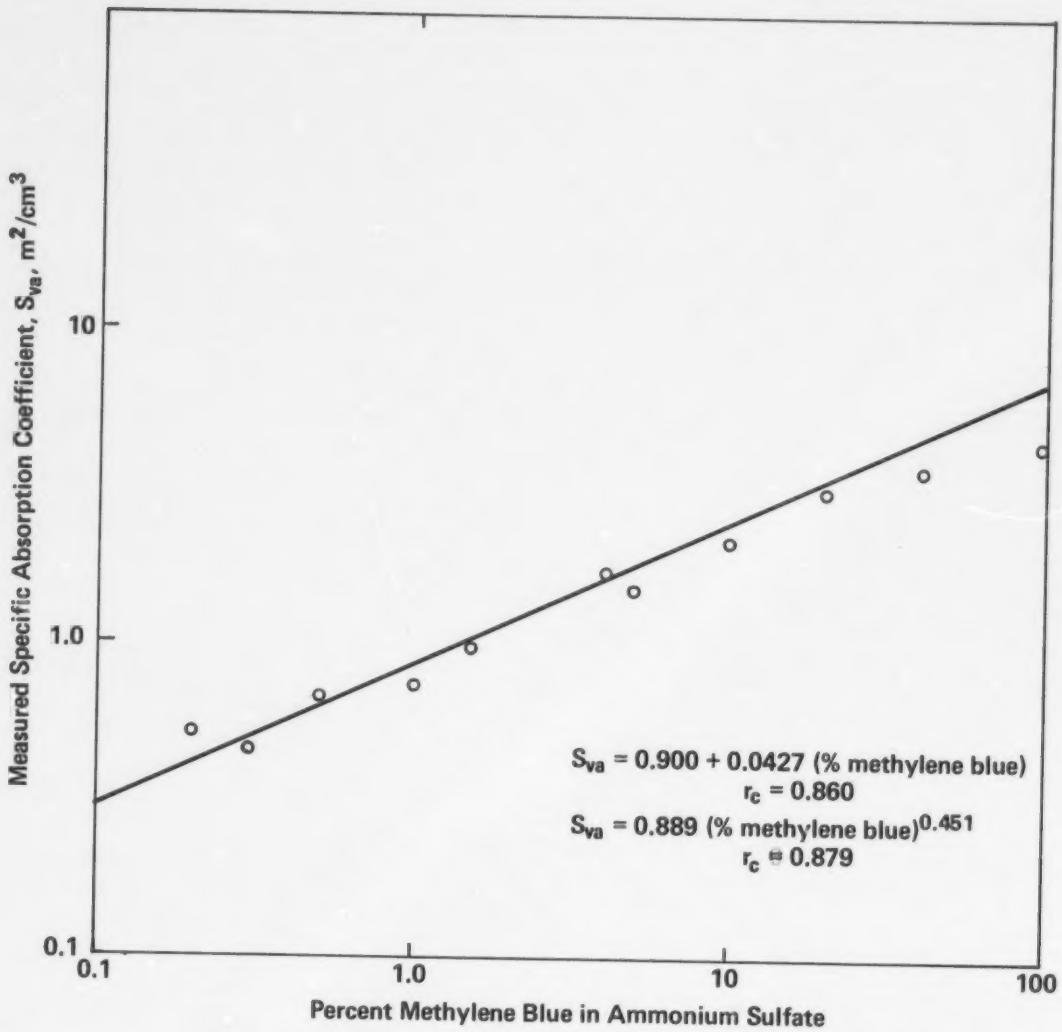

Figure 4. Specific absorption coefficient of methylene blue in ammonium sulfate.

imperfection in the Integrating Plate Method not previously reported by other investigators. This problem is characterized by an erroneous overestimation of absorption probably as a result of light scattering effects. This is the main source of error in the measurement technique and the magnitude of error is dependent on the absorption of the aerosol. Low absorption material will be affected measurably; high absorption aerosol will be affected negligibly. This apparent absorption is seen both in the calibration curve and fly ash absorption analyses (Figure 4). Thus, the fly ash imaginary refractive index determined from the calibration curve is unaffected by the presence of this nonideality.

The calibration aerosol is fairly well characterized in terms of particle size distribution and morphology. These data are presented in Appendix A with a description of particle size measurement techniques used to obtain them.

The Integrating Plate Method has been calibrated with monodisperse, pure methylene blue, 0.8- to 2-μm-diameter aerosol as reported by Weiss et al. (1978). Measurements of methylene blue in this study indicated an accuracy of 25 percent, with gravimetric determinations responsible for the majority of this error. The errors increase to 40 percent for low absorption aerosol, with the optical measurement contributing to most of the error. This error (apparent absorption) may be the result of light scattered and not collected by the photometer detector.

The low carbon fly ash absorption was measured independently using an integrating sphere technique by J. Gillespie of the U.S. Army Atmospheric Services Laboratory, White Sands Missile Range, NM. The results of this interlaboratory comparison are shown in Table 1.

The fundamental difference between the two techniques is that the integrating sphere is a bulk ash absorption measurement while the integrating plate involves individual submicrometer particle absorption. This accounts for most of the dissimilarity in the absorption results. However, the results verify the Integrating Plate Method as an adequate technique for measuring bulk fly ash absorption. The difficulty of the absorption measurement, especially when the absorption is much less than the scattering component, can create errors as great as 40 percent. This is satisfactory

TABLE 1. COMPARISON OF THE ABSORPTION MEASUREMENT BETWEEN THE INTEGRATING PLATE METHOD AND INTEGRATING SPHERE

Ash sample source	Integrating Plate Method	Integrating Sphere Method	Percent difference
Plant MS	0.0055	0.0042	+23.6
Plant K	0.006	0.0087	-45.0
Plant SJ	0.0012	0.0011	+8.3
Plant MS	0.0043	0.0026	+39.5
Plant MS	0.0035	0.0049	-40.0

for opacity modeling because the effect of low absorption on opacity is small. A discussion of opacity modeling appears later in this section.

FLY ASH LIGHT PROPERTIES

Typically, the samples with high F_2O_3 and SO_3 are from the eastern States and the samples with high Ca and low SO_3 are from the western States. All samples, with the exception of Plant N, are from pulverized coal combustion. Plant N was a spreader stoker and exhibited a high concentration of carbon. Spreader stokers usually produce ash with a higher carbon content than pulverized coal combustion and may recycle part of the fly ash back to the grate to improve fuel utilization. In general, the samples represent a good distribution of bituminous coal types.

Real Part of the Refractive Index

Fly ash from 14 different sources with differing chemical compositions and optical properties was analyzed to survey the range and variability of the fly ash refractive index. Table 2 summarizes the fly ash measurements including ash mineral analysis, carbon analysis, and refractive index. The source of each sample is also listed.

The real refractive index of ash is a composite or bulk average of particles spanning a range of indices. This heterogeneity is for the most part compensated for by bulk optical analysis techniques. The sum of the inherent error of the immersion oil technique and the averaging error is approximately 2 percent.

The first step in analysis of the fly ash refractive index data was to compare the real refractive index with particle density. It has been observed in the manufacture of glass that the refractive index is directly related to density. Holloway (1973) describes a theoretical model of glass in which both the refractive index and density are associated with a greater electron density in the material.

A linear correlation was performed between real refractive index and density as shown in Figure 5. The correlation coefficient of 0.8 indicates that 64 percent of the variation is ascribed to the two variables.

The moderate correlation coefficient indicates that the variables are related but other variables are affecting the correlation. The second step

TABLE 2. SUMMARY OF ASH COMPOSITION (%) AND PHYSICAL PROPERTIES

Source	SiO_2	Al_2O_3	Fe_2O_3	TiO_2	P_2O_5	CaO	MgO	Na_2O	K_2O	SO_3	C	Density (g/cm^3)	Refractive index
Plant SJ	46.8	28.07	3.8	1.3	7.2	4.81	1.45	4.36	0.98	1.74	0.4	2.1	1.55 -0.002i
Plant MS	28.27	34.11	13.69	1.29	ND	1.11	2.55	0.32	2.94	3.95	0.91	2.25	1.575 -0.005i
Plant K	49.29	25.07	4.72	0.89	22.0	6.46	4.75	0.65	1.42	0.74	0.94	2.3	1.58 -0.0076i
Plant C	40.22	28.21	24.71	0.62	ND	5.22	1.16	0.2	0.73	0.285	1.5	2.5	1.595 -0.012i
Plant DE	31.82	25.98	38.26	0.74	ND	1.26	0.98	0.2	1.59	0.35	7.5	2.45	1.575 -0.014i
Plant H	32.81	18.61	7.04	1.60	0.91	26.74	6.94	1.31	0.30	2.46	0.4	2.635	1.61 -0.0012i
Plant GN	49.7	19.0	6.74	0.9	0.77	16.4	3.0	0.36	1.78	1.0	0.6	2.4	1.575 -0.0013i
Plant N	27.9	14.4	1.19	0.4	ND	0.85	0.45	0.1	ND	ND	33.5	2.0	1.535 -0.029i
Plant S	39.7	16.6	21.5	0.74	ND	7.6	1.0	0.86	ND	ND	1.4	2.55	1.57 -0.0005i
SORI MG	40.8	22.7	11.6	1.63	ND	0.91	1.56	0.85	3.25	ND	8.7	2.55	1.595 -0.016i
SORI 121	38.8	21.6	4.8	1.9	1.4	22.7	4.0	1.13	0.7	1.7	0.7	2.6	1.59 -0.0018i
SORI 123	58.5	23.4	4.3	1.7	0.3	5.2	0.9	1.38	1.1	0.7	2.2	2.45	1.56 -0.0044i
SORI 124	50.4	19.5	19.3	1.6	0.3	4.7	1.0	0.47	2.7	1.5	1.2	2.68	1.58 -0.0025i
SORI 143	54.5	31.5	4.8	2.8	0.1	1.2	0.8	0.22	2.7	0.2	2.45	2.2	1.56 -0.0036i

ND = Not detected.

SORI = Samples provided by Southern Research Institute.

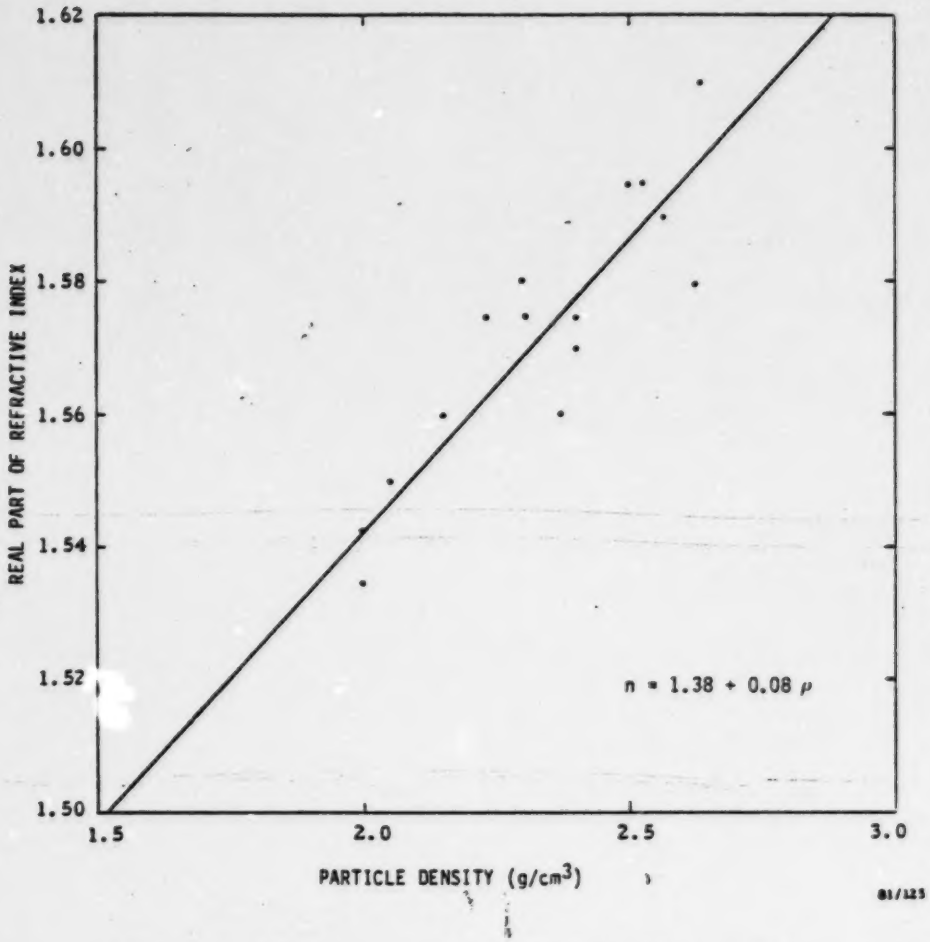

Figure 5. Effect of particle density on the real refractive index.

was to again use information from the glass literature. Morey (1938) suggests an empirical approach to relate refractive index, density, and the composition of glass. A quantity called the specific refractivity was defined by several formulas proposed by various investigators:

1. Specific refractivity = $(n' - 1)/\rho$.
2. Specific refractivity = $(n'^2 - 1)/(n'^2 + 2)\ 1/\rho$.
3. Specific refractivity = $(n'^2 - 1)/(n + 0.4)\ 1/\rho$.
4. Specific refractivity = $(\log n')/\rho$.

A regression equation is defined by:

$$\text{Specific refractivity} = B_0 + B_1(X1) + \ldots + B_N(XN) \qquad (8)$$

where

B's = best-fit coefficients

X's = the percentages by weight of various components such as SiO_2 or CaO.

The glass data discussed by Morey (1938) were for well-characterized three-component systems. Here the application of this concept is extended to a multicomponent system of a combustion origin.

The results of the regression analysis are reported in Table 3. The various specific refractivity expressions were tried. The first expression provided the equation with the best prediction. It is also the simplest to use. (Morey reported the same conclusions for glass.) It should also be noted that the values not determined were set to 0 for the regression. The square of correlation coefficient for the regression equation of 0.82 indicates that only 18 percent of the variability in the data is not described by the equation. The standard error of estimate of 0.01 indicated an error of 6 percent at the mean specific refractivity. The regression equation is:

$$\begin{aligned}(n'-1)/\rho = 0.263 &- 0.000525(\%SiO_2) + 0.00144(\%Al_2O_3) \\ &- 0.001198(\%Fe_2O_3) - 0.00803(\%TiO_2) \\ &- 0.000819(\%CaO) + 0.000139(\%MgO) \\ &- 0.000182(\%Na_2O) + 0.00231(\%K_2O)\ .\end{aligned} \qquad (9)$$

TABLE 3. MULTILINEAR REGRESSION ANALYSIS OF SPECIFIC REFRACTIVITY AND ASH COMPOSITION

$y = (n'-1)/\rho$

$X_1 = \%SiO_2$
$X_2 = \%Al_2O_3$
$X_3 = \%Fe_2O_3$
$X_4 = \%TiO_2$
$X_5 = \%CaO$
$X_6 = \%MgO$
$X_7 = \%Na_2O$
$X_8 = \%K_2O$

(partial correlation coefficients):

	X1	X2	X3	X4	X5	X6	X7	X8
X1	1.00000	-0.03002	-0.21416	0.21422	0.12364	-0.25539	0.16322	0.16145
X2	-0.03002	1.00000	0.34676	0.40604	-0.50730	0.42308	0.29603	0.07082
X3	-0.21416	0.34676	1.00000	-0.42777	0.34660	-0.42608	-0.25461	0.24649
X4	0.21422	0.40604	-0.42777	1.00000	0.53567	-0.37527	-0.01269	0.53956
X5	0.12364	-0.50730	0.34660	0.53467	1.00000	0.85466	0.08312	-0.50620
X6	-0.25539	0.42308	-0.42608	-0.37527	0.85466	1.00000	-0.07357	0.37243
X7	0.16322	0.29603	-0.25461	-0.01269	0.08312	-0.07357	1.00000	-0.26056
X8	0.16145	0.07082	0.24649	0.53956	-0.50620	0.37243	-0.26056	1.00000

Term	Value	Standard error	t-ratio	Degrees of freedom
B0	0.2625365	0.0213687	12.2860	5
B1	-0.0005251	0.0003738	-1.4046	5
B2	0.0014413	0.0007568	1.9044	5
B3	-0.0011976	0.0003716	-3.2227	5
B4	-0.0080331	0.0076354	-1.0521	5
B5	-0.0008187	0.0008814	-0.9289	5
B6	0.0001387	0.0033645	0.0412	5
B7	-0.0001819	0.0031461	-0.0578	5
B8	-0.0023103	0.0043762	-0.5279	5

Composition of the Variance of Y:

Source		Sum of squares	Degrees of freedom	Mean sum of squares
Total		0.00311426	13	0.00023956
Regression		0.00255169	8	0.00031896
Residual		0.00056257	5	0.00011251
Number of Observations	14.00000000			
R^2	0.81935677			
$\bar{R}^2$	0.53032761			
Standard Error of the Estimate	0.01060726			
F-Statistic (8 & 5 D.F.)	2.83485848			

			95% Confidence interval using observed X's	
Actual Y	Predicted Y	Residual	Lower	Upper
0.262	0.257	0.005	0.219	0.295
0.256	0.263	-0.007	0.227	0.298
0.252	0.252	0.000	0.215	0.289
0.238	0.242	-0.004	0.208	0.275
0.235	0.227	0.008	0.193	0.261
0.232	0.229	0.003	0.193	0.265
0.240	0.231	0.008	0.195	0.268
0.268	0.263	0.004	0.226	0.301
0.224	0.228	-0.004	0.196	0.260
0.233	0.239	-0.005	0.205	0.272
0.227	0.232	-0.006	0.199	0.266
0.229	0.240	-0.011	0.208	0.272
0.216	0.218	-0.002	0.185	0.251
0.255	0.244	0.011	0.208	0.280

The use of Equation 9 requires the same precautions that are applied to any empirical relationship. Care should be taken with data that lie outside the data base and the regression equation should be modified as new data become available.

The implications of this result are significant. First, the specific refractivity can be predicted with good accuracy from the mineral analysis of an ash. Perhaps ashes that may be troublesome from an opacity standpoint can be identified before the power plant is designed. Second, the interdependence of density and refractive index eliminates one variable required to predict opacity. The variability of opacity for a given particle size distribution can be estimated more accurately than before.

Imaginary Part of the Refractive Index

The most important variable for fly ash absorption is the graphitic carbon content. The range of carbon content varied from 0.4 to 33.5 percent, with most of the samples containing less than 2 percent. The high carbon content ashes may indicate inefficient boiler operation such as uneven combustion or improper fuel/air ratios. The highest carbon ash was found at Plant N, a spreader stoker.

The light absorption of fly ash as a function of graphitic carbon, shown in Figure 6, resembles the calibration curve using methylene blue ammonium sulfate aerosol. The apparent absorption is approximated by extrapolating the regression line to 0 percent carbon. This indication of absorption where little is expected is observed for the nonabsorbing ammonium sulfate interferences. This apparent, not real, absorption appears to be a repeatable phenomenon of the Integrating Plate Method. The calibration curve described earlier was used to compensate for this nonideality and an accurate imaginary refractive index can still be obtained. The linearity of low absorption ashes with a high correlation of 0.97 to carbon content is also similar to the linearity of the low absorbing, low concentration methylene blue in ammonium sulfate aerosol calibration.

The curves in Figure 6 should be extrapolated to other fly ash samples with caution. The tendency of the Integrating Plate Method is to underpredict the actual absorption for high carbon ashes so that the errors from

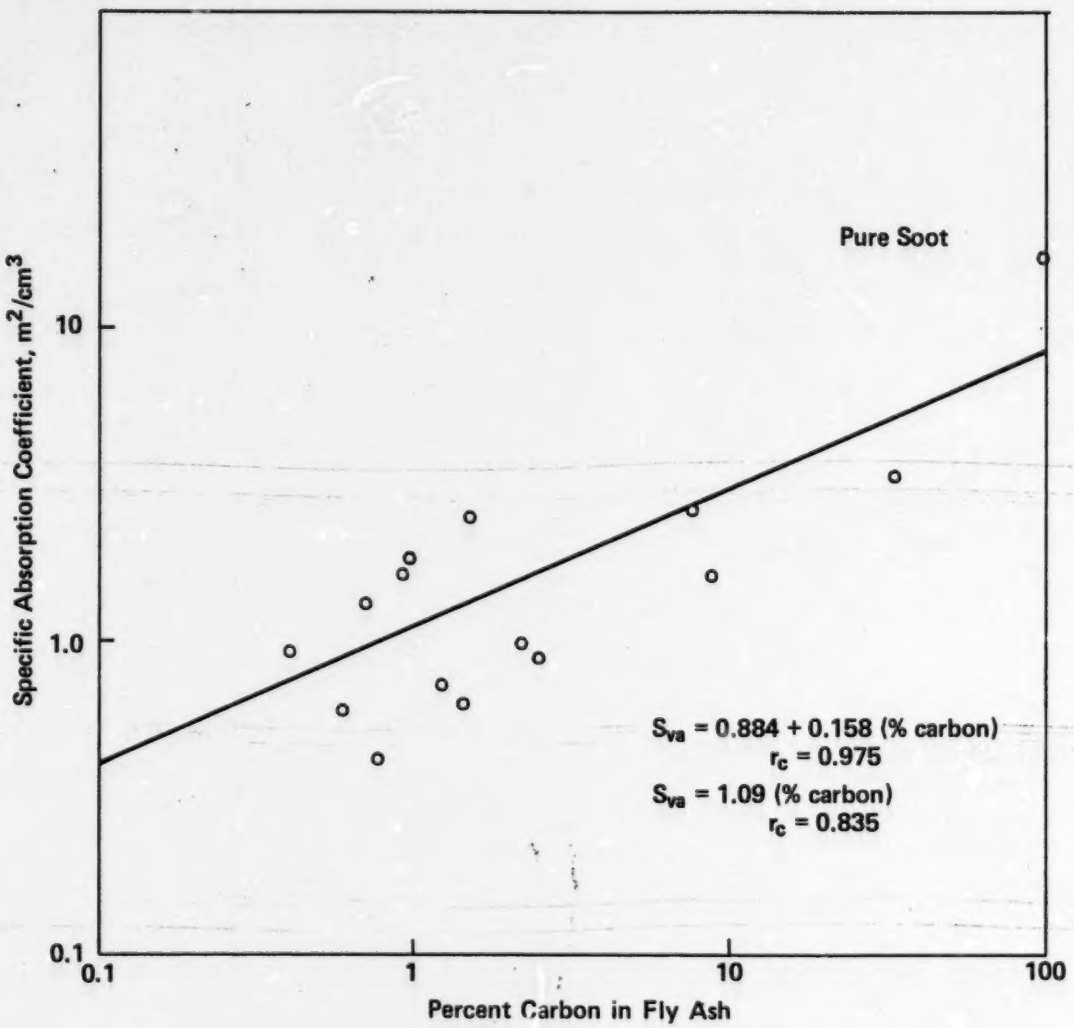

Figure 6. Specific absorption coefficient of fly ash as a function of carbon content.

scattered light would be reduced. The coarse fraction of ash was removed before deposition of the fine particles onto the filter for absorption measurement. If part of the carbon is present as large-diameter char rather than soot, it will be excluded from the measurement. Therefore, the carbon content measured on the bulk ash may not be representative of the ash characterized by the Integrating Plate Method.

This fly ash carbon heterogeneity also may cause problems in the low absorption cases where individual black particles (>100 μm) were visible in the ash hopper sample. In situ ash sample collection with a precutter would eliminate this source of error. Then the identical sample with submicrometer material could be used for both carbon and light absorption measurements.

Since soot emissions from coal-fired boilers may be important for stack opacity, soot light absorption was measured using the Integrating Plate Method. The soot was generated at the First International Workshop on Light Absorption of Aerosols by combustion of propane. Figure 7 shows a microphotograph of the soot with its distinctive chain-like structure. The soot size distribution is shown in Figure 8.

The determination of the imaginary refractive index for soot from the Integrating Plate Method measurements was approximated by Weiss (Equation 5).

The assumptions are a homogeneous aerosol of assumed density (1.8 g/cm^3) and real refractive index (1.45), fine particles, and a single wavelength. The imaginary refractive index for soot using this formula is 0.9 and the mass absorption coefficient b_{abs} is 9.6 m^2/g. The apparent absorption caused by scattered light does not substantially affect the measured absorption of highly absorbing aerosol because it constitutes a small percentage (<5 percent) of the total absorption.

In Figure 9, the imaginary refractive index obtained for each fly ash sample is compared to the percent carbon content of the fly ash. The pure soot case was not included because of bias for highly absorbing material, and the absorption coefficient offset due to scattering has been removed by the use of the calibration aerosol. Therefore, this curve should provide reasonable estimates of imaginary refractive indices from ash carbon analysis.

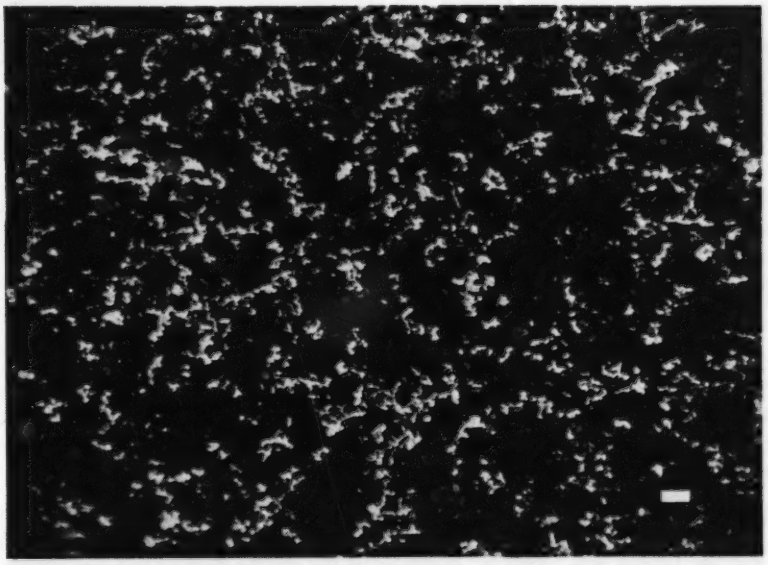

81-171

Figure 7. Microphotograph of soot aerosol (4000X).

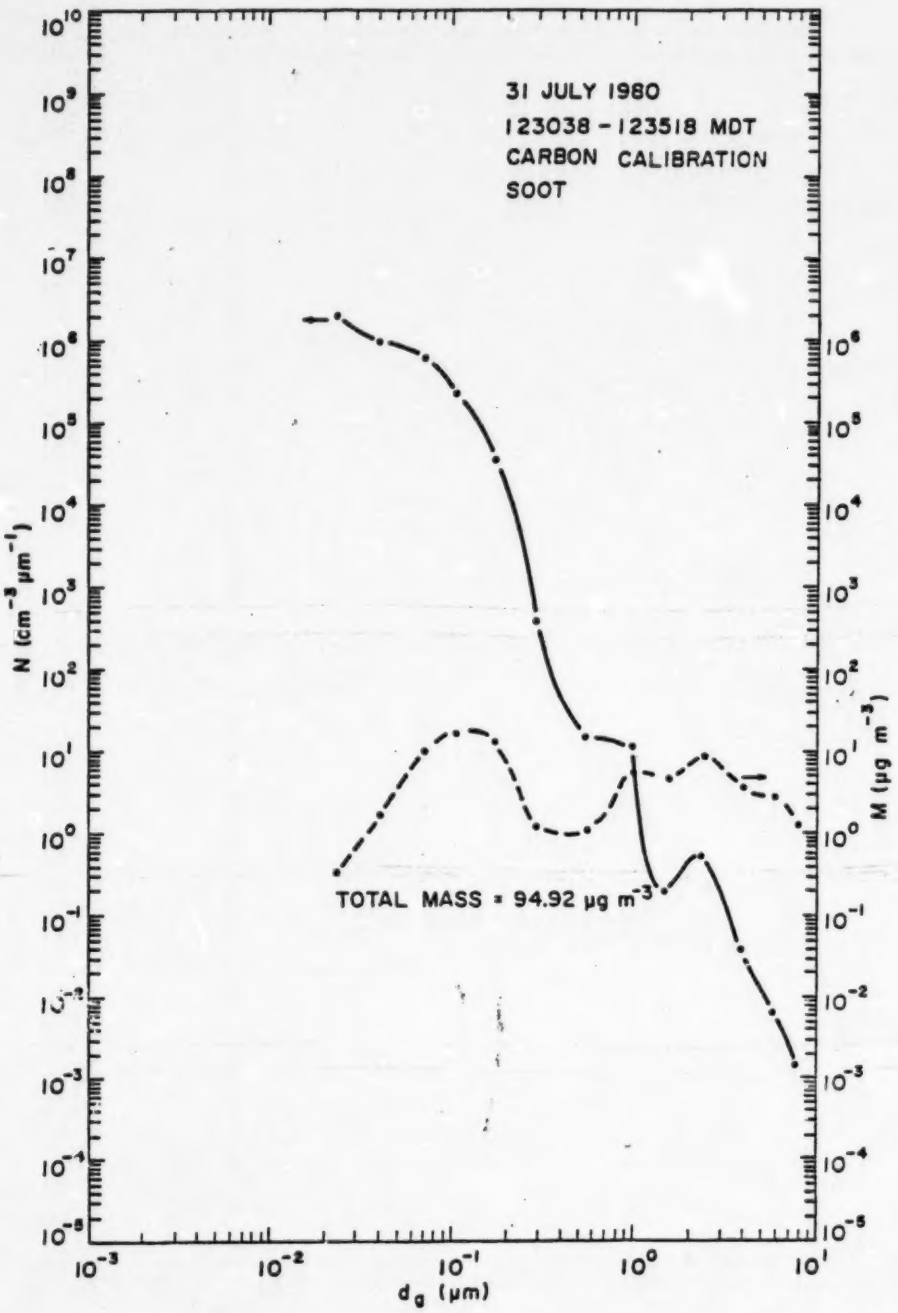

Figure 8. Aerosol size distribution of soot particles.

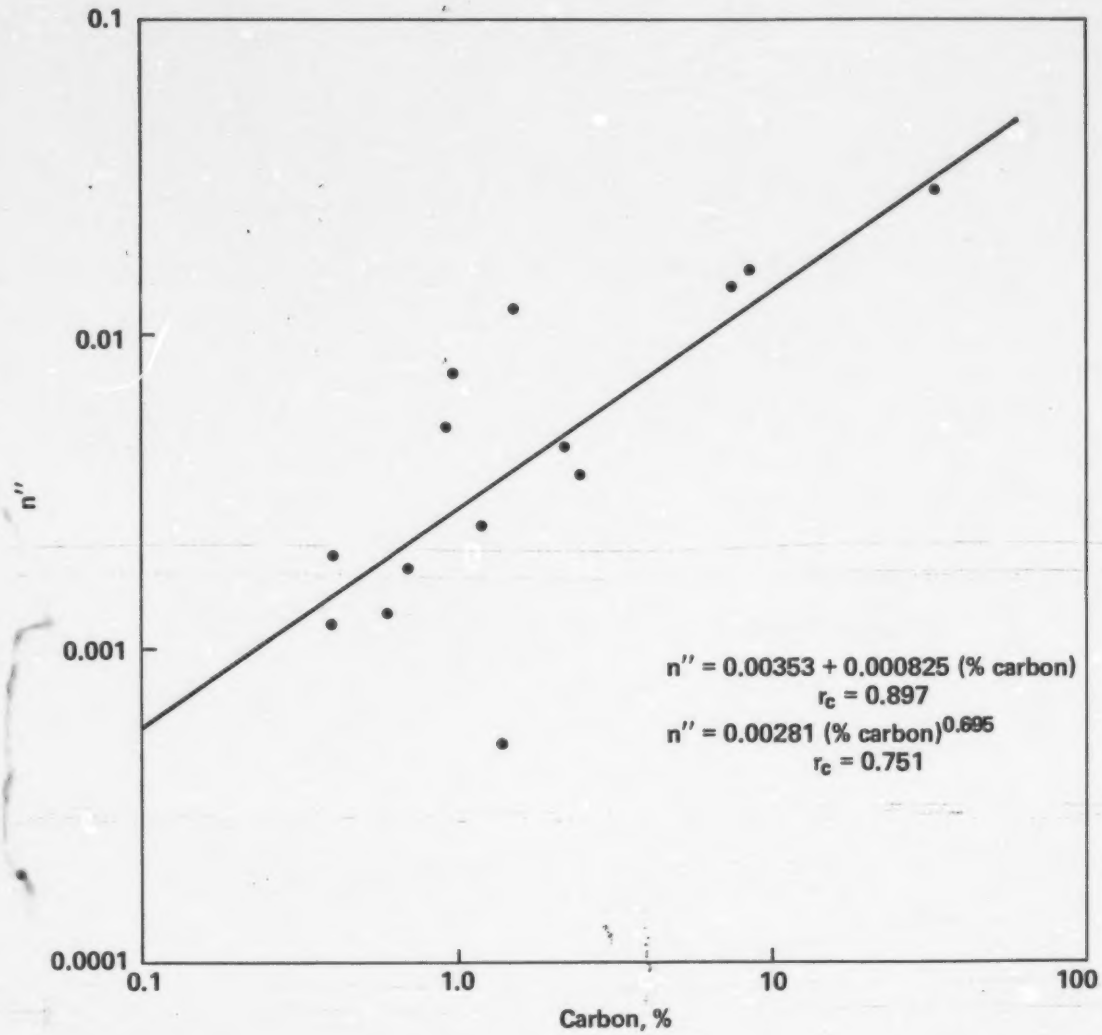

Figure 9. Imaginary refractive index of fly ash as a function of carbon content.

SIGNIFICANCE OF THE MATERIAL PHYSICAL PROPERTIES ON IN-STACK OPACITY

The primary goal of this study is to estimate the importance of particle physical properties on the resulting in-stack plume opacity. Three cases are of interest: (1) the range of opacities expected from the coupled behavior of real refractive index and density; (2) the importance of absorbing refractive index under typical conditions; and (3) the absorbing refractive index under upset conditions when the production of soot is much greater than normal. The computer programs described by Cowen et al. (1983) for a Radio Shack TRS-80 computer were used in this part of the study.

The range of real refractive index and density was evaluated as a function of particle diameter. The results are shown in Figure 10. The mass extinction coefficient (m^2/g) is used as an indicator of opacity. The opacity can be computed with the modified Beer-Lambert Law.

$$I/I_o = \exp(-S_m M L) \quad (8)$$

where S_m is the mass extinction coefficient. Surprisingly, the computed opacity decreases when the real part of the refractive index increases, because the real part of the refractive index increases with increasing particle density. Since the opacity is inversely proportional to the particle density (at low opacities), the effect of the refractive index on opacity is substantially diminished. The preliminary modeling analysis shows that the ratio of the two ash properties, refractive index and particle density, determines their effect on in-stack opacity.
The variation in real refractive index/density results in a range of ±20 percent variation in the mass extinction coefficient. The range of variability depends on the size distribution in the particular source. However, the maximum variability is in the particle range greater than 0.5 μm diameter, the range for fly ash emissions. Therefore, the refractive index/density can be significant for fly ash and should be included in efforts to predict opacity.

The second case study was based on a hypothetical particle size distribution of fly ash, which represents the emissions from a pulverized coal-fired boiler well controlled with an electrostatic precipitator. The opacity was computed with one of the measured refractive indices as a

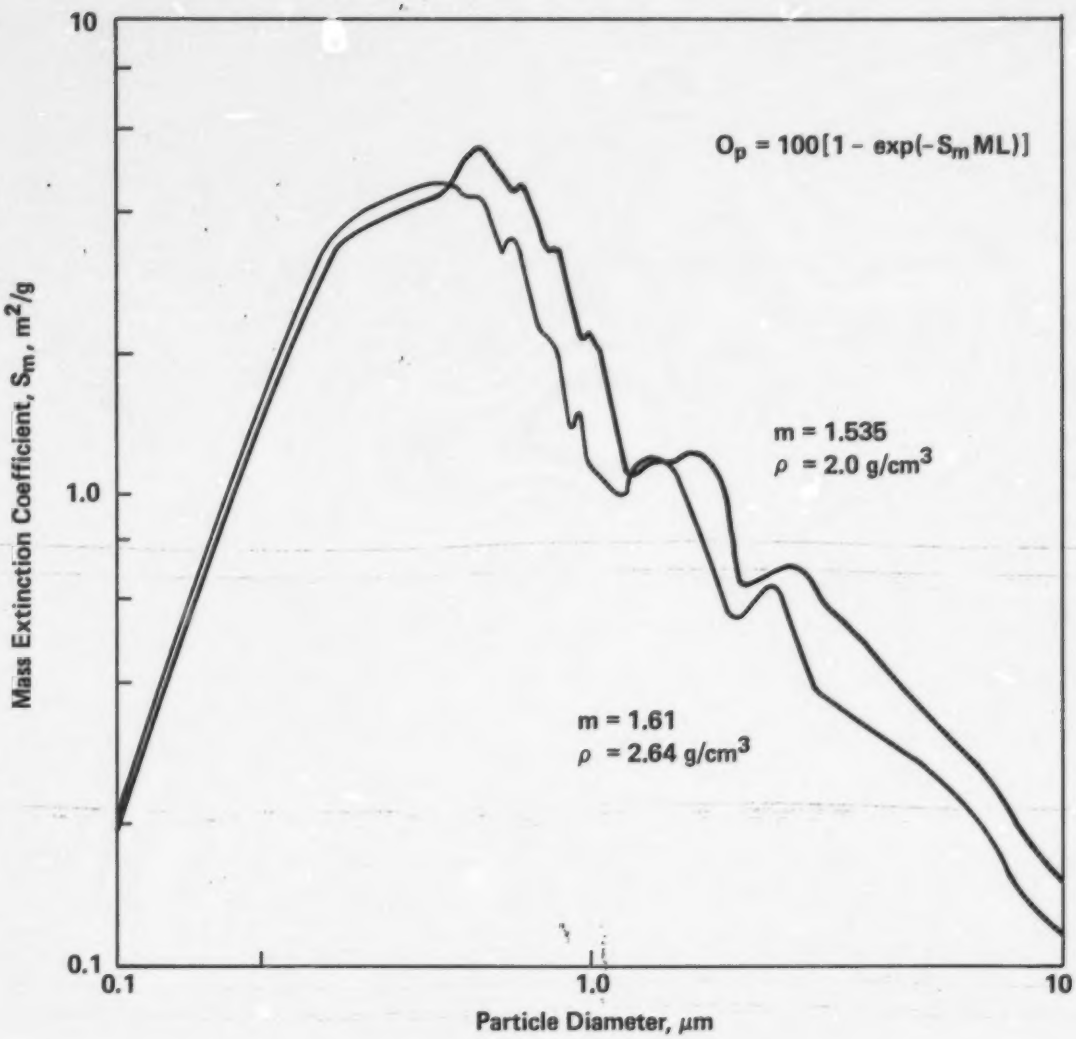

Figure 10. The effect of the extremes of refractive index and density on the mass extinction coefficient for monodisperse particles.

reference and then recomputed with the absorbing refractive index set to 0. The results in Table 4 indicate that for these conditions of particle size distribution, the effects of absorbing refractive index are insufficient. The importance of the absorbing refractive index is strongly dependent on particle size. For large particles (>5 μm), the light extinction is independent of the refractive index.

The sensitivity of opacity to the absorbing refractive index may be important if the particle size distribution is altered by changes in the combustion conditions.

The properties of soot affecting both the refractive index/density and the particle size distribution were evaluated in the final case. The same size distribution assumed for fly ash was mixed with size distribution of soot shown in Figure 8 to make a 30-percent carbon mixture. The results of the computations are given in Table 5. As indicated, the opacity can increase dramatically.

Soot has a much larger mass extinction coefficient than fly ash. Therefore, the opacity can be greatly increased by the presence of soot. The relationship of opacity and mass concentration may be altered under conditions of poor combustion. Plume opacity under these conditions is a conservative indicator of an increase in mass emission.

TABLE 4. COMPUTED EFFECTS OF ABSORBING REFRACTIVE INDEX ON PLUME OPACITY

Refractive index density combination	Refractive index	Particle density g/cm^3	Specific volume extinction coefficient S_v m^2/cm^3	Computed opacity, %[a]
High refractive index and density absorbing ash	1.61 - 0.029i	2.64	2.70	9.74
High refractive index and density nonabsorbing ash	1.61 - 0i	2.64	2.76	9.91
Low refractive index and density absorbing ash	1.535 - 0.029i	2.0	2.73	12.76
Low refractive index and density nonabsorbing ash	1.535 - 0.0i	2.0	2.81	13.10

[a]The particle mass concentration is assumed to be 0.02 g/m^3. The stack diameter is 5 m. The particle size distribution is:

Particle diameter (μm)	Cumulative mass function
0.5	0.0211
0.6	0.0641
0.8	0.126
1	0.2176
1.5	0.352
2	0.496
3	0.61
4	0.699
6	0.772
8	0.842
10	0.912
15	0.99

The mass mean diameter equals 2.4 μm. The geometric standard deviation is 2.5.

TABLE 5. EFFECT OF SUBMICROMETER SOOT ON OPACITY

Case	Refractive index	Particle density	Specific volume extinction coefficient S_v, m^2/cm^3	Mass extinction coefficient S_m m^2/g	Computed opacity, %
Last case from Table 4	1.535 - 0.0i	2.0	2.81	1.40	13.1
100% Soot	1.96 - 0.66i	1.8	17.28	9.60	61.7
5% Soot	--	2.0	3.62	1.81	16.6
10% Soot	--	1.98	4.39	2.22	19.9
20% Soot	--	1.96	5.96	3.04	26.2

$$O_p = 100 [1 - \exp (-S_m ML)$$

$$Sm = \frac{S_{vash}}{\rho_{ash}} F_{ash} + \frac{S_{vsoot}}{\rho_{soot}} F_{soot}$$

The size distribution for ash in Table 5 is assumed. The soot will be typically 0.2 μm in diameter and the optical effects are additives.

REFERENCES

Bickelhaupt, R. E. (1979): A Technique for Predicting Fly Ash Resistivity. EPA-600/7-79-204.

Clarke, A. D. (1982): Effects of Filter Internal Reflection Coefficient on Light Absorption Measurements Made Using the Integrating Plate Method. Applied Optics, 21, 3021-3031.

Cowen, S. J., D. S. Ensor, and L. E. Sparks (1980): TI-59 Programmable Calculator Programs for In-Stack Opacity, Venturi Scrubbers, and Electrostatic Precipitators. EPA-600/8-80-024.

Cowen, S. J., D. S. Ensor, and L. E. Sparks (1983): Basic In-Stack Opacity Programs: User and Programmer Manual. In press. U.S. EPA Environmental Research Laboratory, Research Triangle Park, NC.

Ensor, D. S. (1972): Smoke Plume Opacity Related to the Properties of Air Pollutant Aerosols. Ph.D. Dissertation, University of Washington, Seattle.

Fisher, G. L., B. A. Prentice, D. Silberman, J. M. Ondov, A. H. Biermann, R. C. Ragaini, and A. R. McFarland (1978): Physical and Morphological Studies of Size Classified Coal Ash. Environ. Sci. Technol., 12, 447-451.

Gluskoter, H. J., R. R. Ruch, W. G. Miller, R. A. Cahill, G. B. Dreher, and J. K. Kuhn (1977): Trace Elements in Coal: Occurrence and Distribution. EPA-600/7-77-064.

Hindmann, E. H., R. D. Horn, and W. G. Finnegan (1982): Particle Generation, Transport, and Characterization at the First International Workshop on Light Absorption by Aerosol Particles. Applied Optics, 21, 403-412.

Holloway, D. G. (1973): The Physical Properties of Glass. Wykeham Publications Ltd., London, p. 102.

Lin, C., M. Baker, and R. J. Charlson (1973): Absorption Coefficient of Atmospheric Aerosol: A Method for Measurement. Appl. Optics, 12, 1356-1363.

Morey, G. W. (1938): The Properties of Glass. Reinhold, New York, NY, 387-391.

McCrone, W. C., R. G. Draftz, and J. G. Delly (1967): The Particle Atlas. Ann Arbor Science Publishers, Ann Arbor, MI.

Nolan, J. L. (1977): Measurement of Light Absorbing Aerosols From Combustion Sources. M.S. Thesis, University of Washington, Seattle, WA.

Volz, F. E. (1973): Infrared Optical Constants of Ammonium Sulfate, Sahara Dust, Volcanic Pumice, and Fly Ash. Appl. Optics, 12, 564-568.

Weiss, R. E., A. P. Wagoner, R. J. Charlson, D. L. Thorsell, J. S. Hall, and L. A. Riley (1978): Studies of the Optical, Physical, and Chemical Properties of Light Absorbing Aerosols. Presented at Conference on Carbonaceous Particles in the Atmosphere, Berkeley, CA, 20-22 March.

Weiss, R. E. (1980): The Optical Absorption Properties of Suspended Particles in the Lower Troposphere at Visible Wavelengths. Ph.D. Dissertation, University of Washington, Seattle, WA.

APPENDIX A

CALIBRATION AEROSOL DATA

Particle size distribution was measured using a Thermo Systems, Inc., electrical aerosol analyzer for particles below 0.5 μm, a Particle Measurement Systems Active Scattering Probe (ASAP-X) for particles from 0.09 to 3 μm, and a scanning electron microscope. These aerosols were generated at Colorado State University's and MRI's aerosol laboratories. Figures A-1 through A-22 provide microphotographs and the mass and number aerosol size distributions for pure ammonium sulfate and ammonium sulfate with the following concentrations of methylene blue: 0.2, 0.3, 0.5, 1.5, 4, 5, 10, 20, 40, and 100 percent.

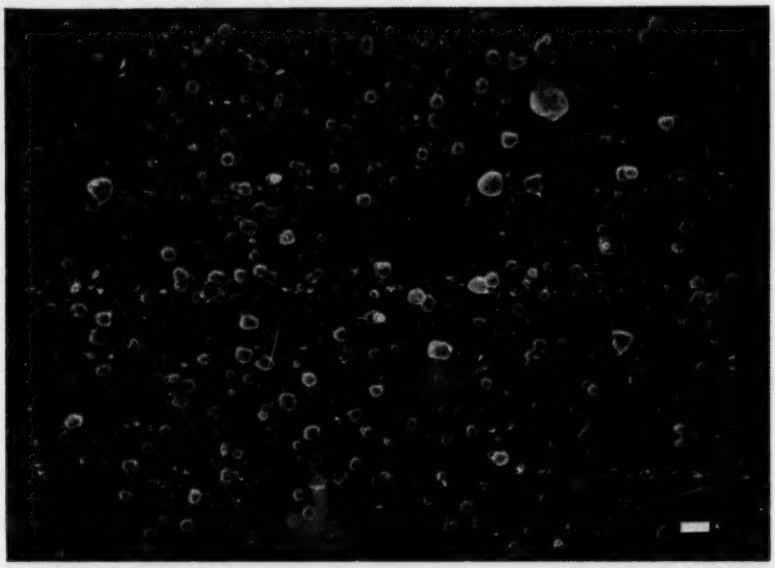

Figure A-1. Microphotograph of ammonium sulfate aerosol (4000X).

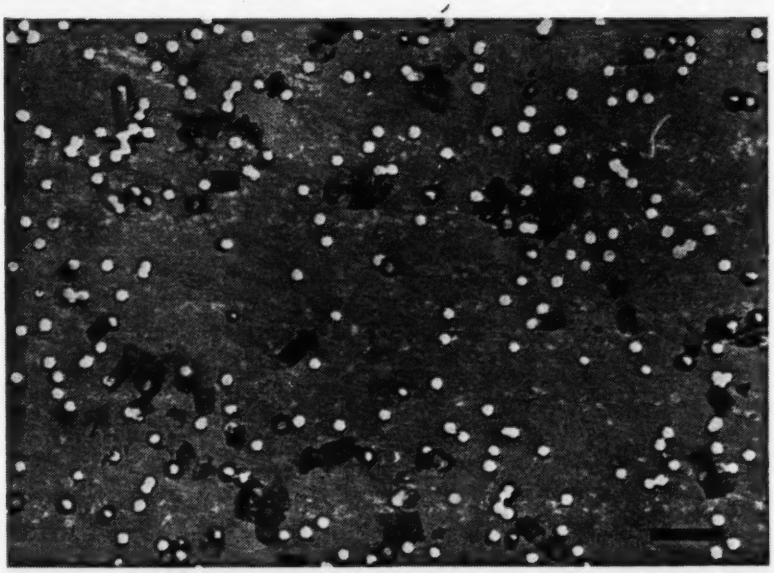

81-172

Figure A-2. Microphotograph of ammonium sulfate aerosol with 0.2% methylene blue (10,750X).

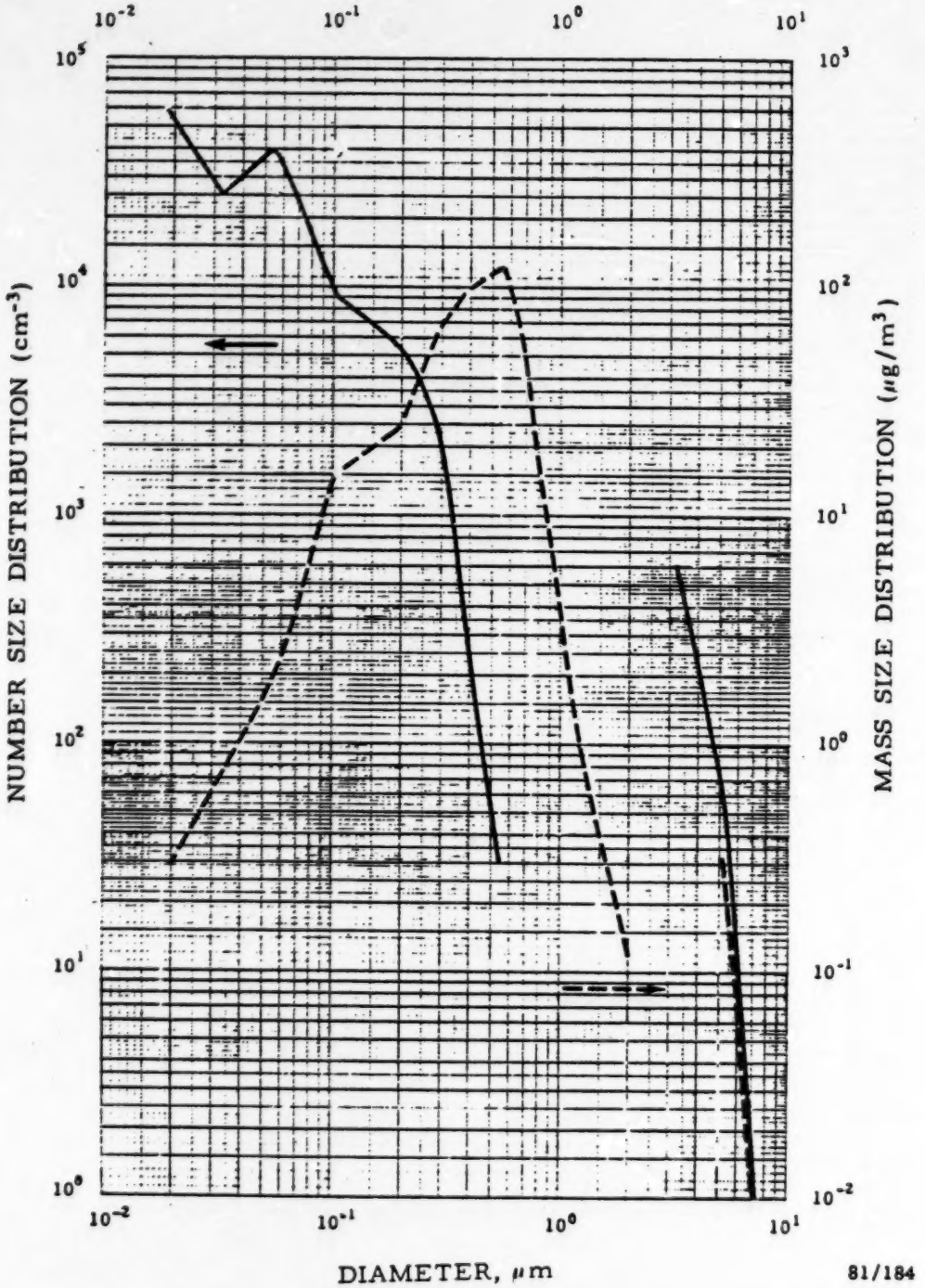

Figure A-3. Aerosol size distribution of ammonium sulfate aerosol.

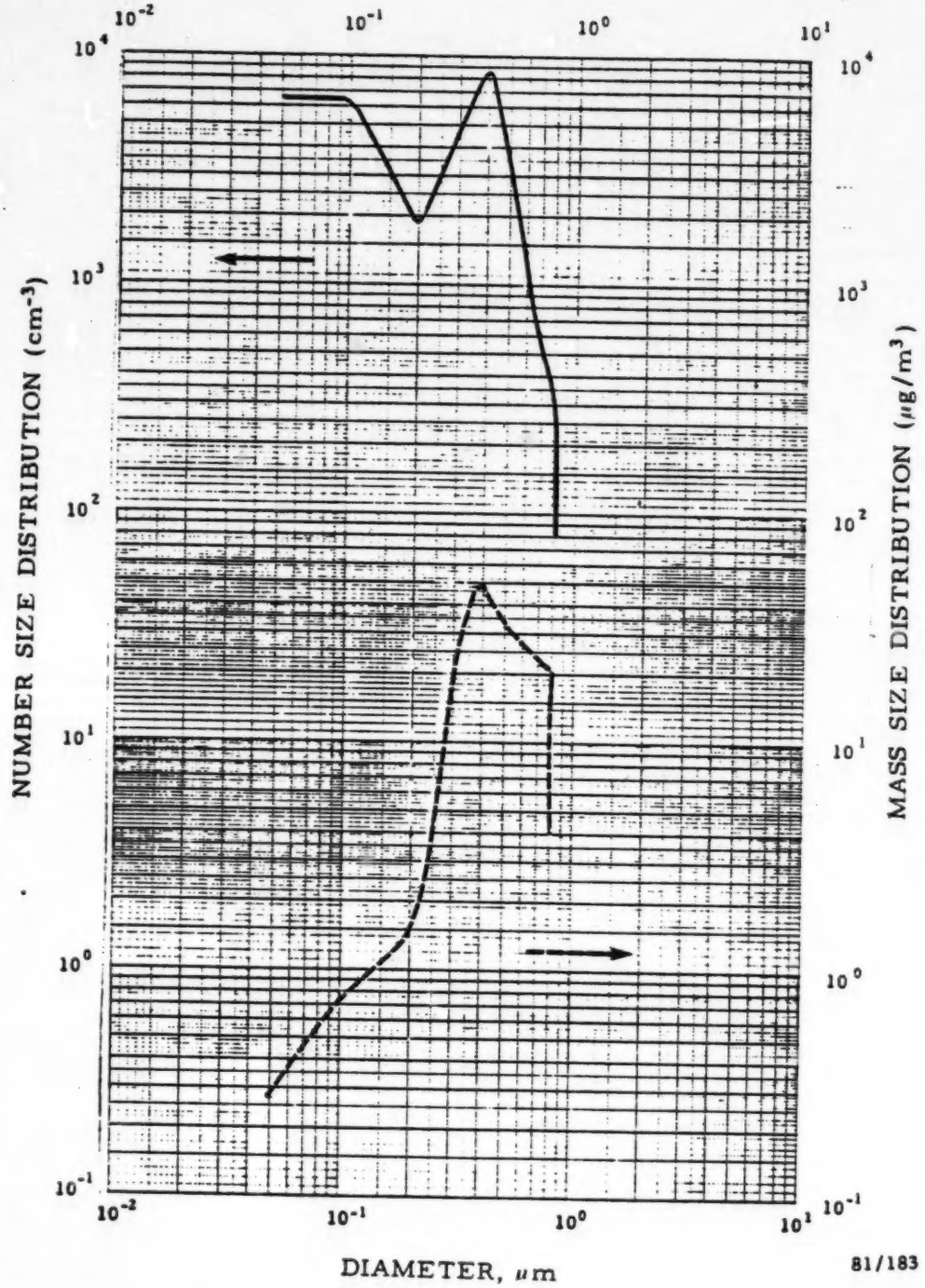

Figure A-4. Aerosol size distribution of ammonium sulfate aerosol with 0.2% methylene blue.

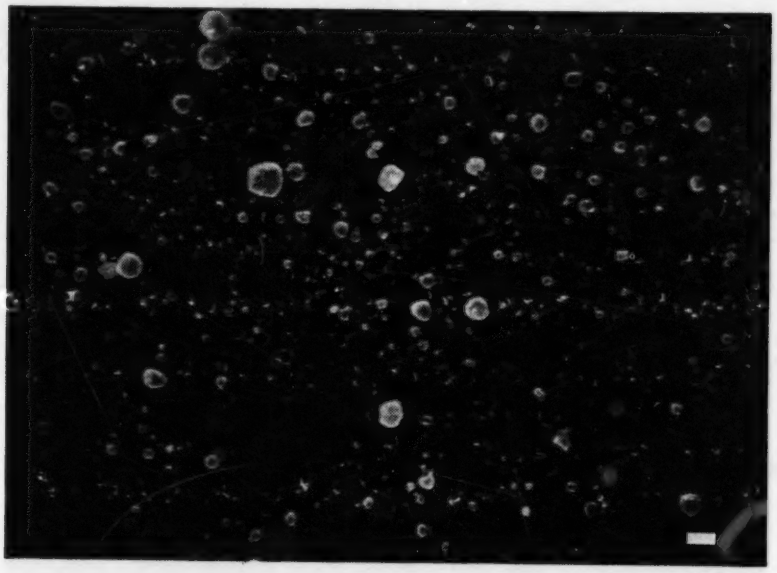

Figure A-5. Microphotograph of ammonium sulfate aerosol with 0.3% methylene blue (4000X).

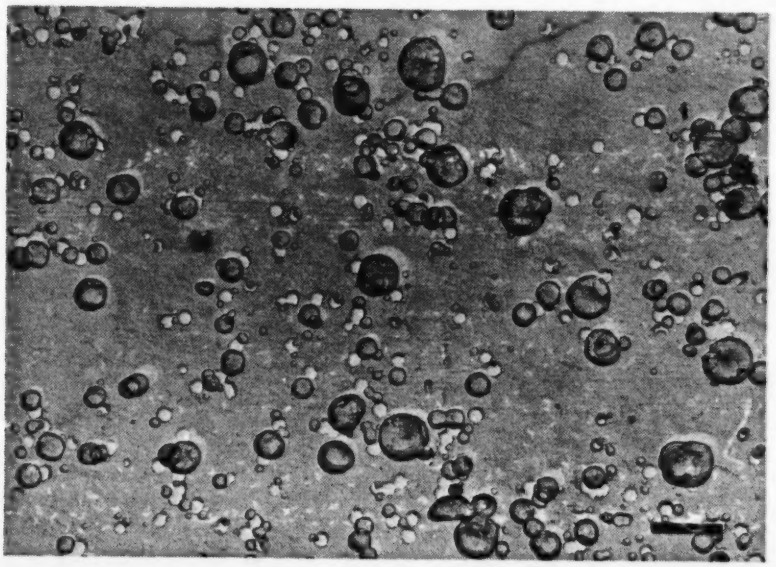

81-173

Figure A-6. Microphotograph of ammonium sulfate aerosol with 0.5% methylene blue (10,750X).

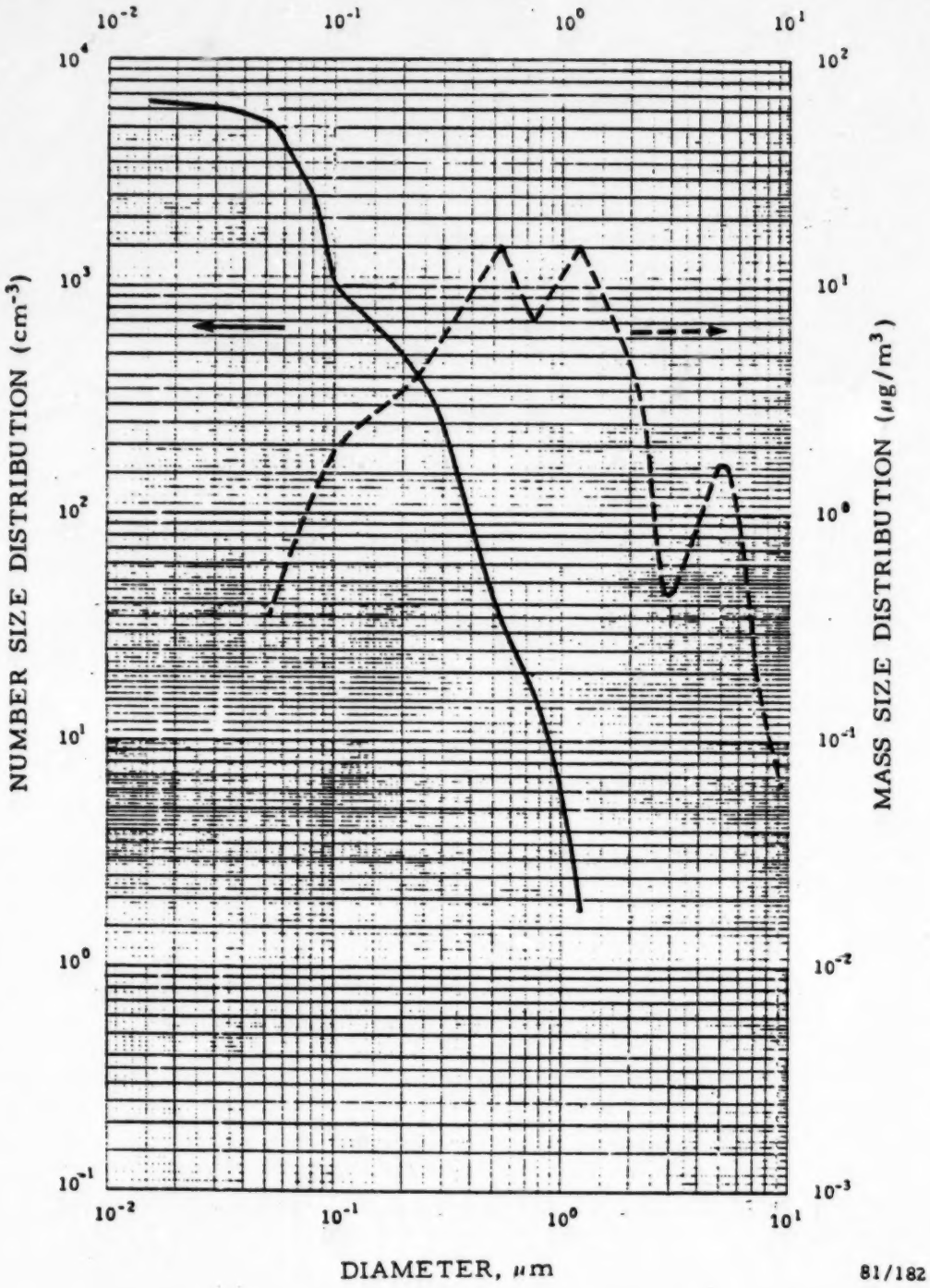

Figure A-7. Aerosol size distribution of ammonium sulfate aerosol with 0.3% methylene blue.

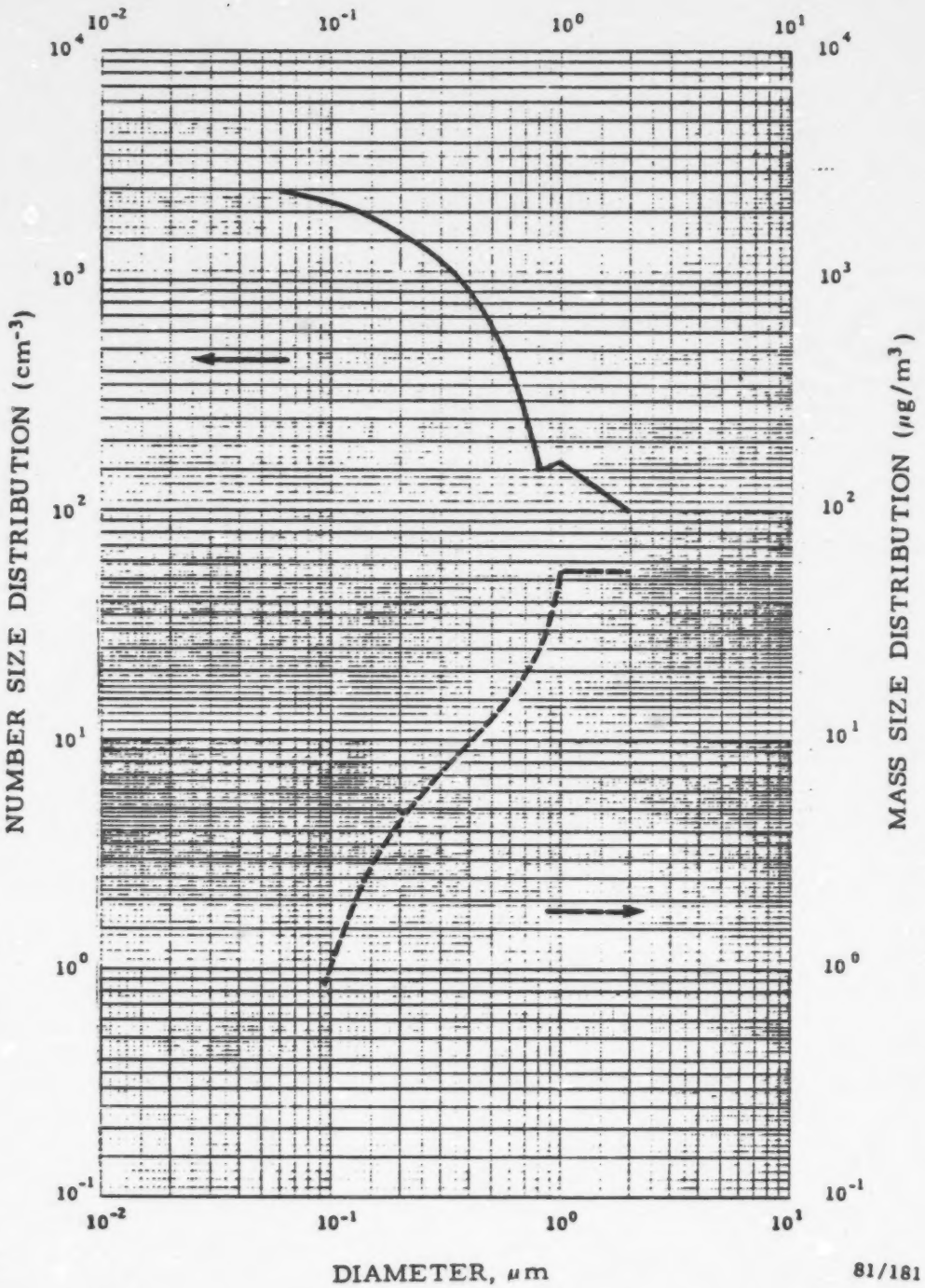

Figure A-8. Aerosol size distribution of ammonium sulfate aerosol with 0.5% methylene blue.

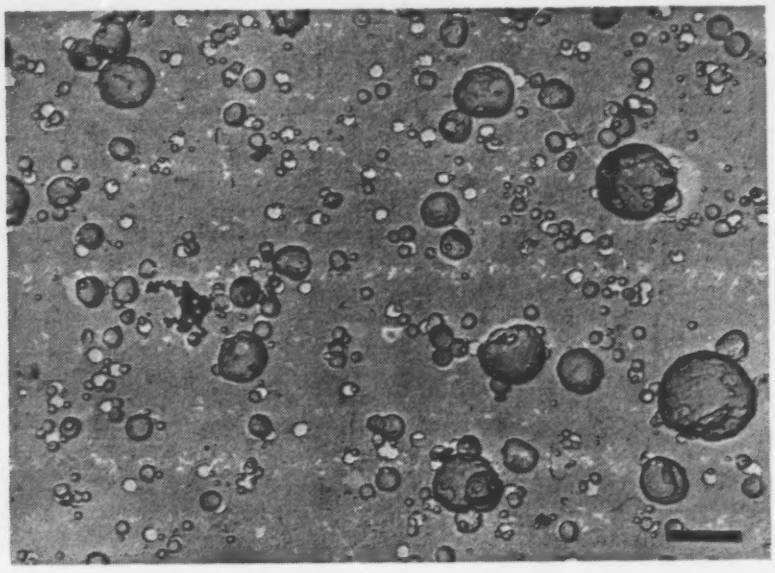

Figure A-9. Microphotograph of ammonium sulfate aerosol with 1.5% methylene blue (10,750X).

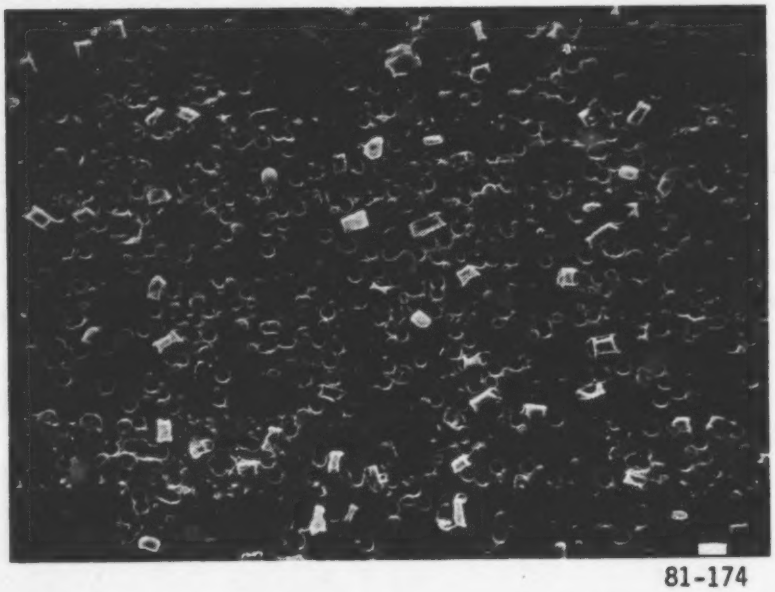

81-174

Figure A-10. Microphotograph of ammonium sulfate aerosol with 4% methylene blue (4000X).

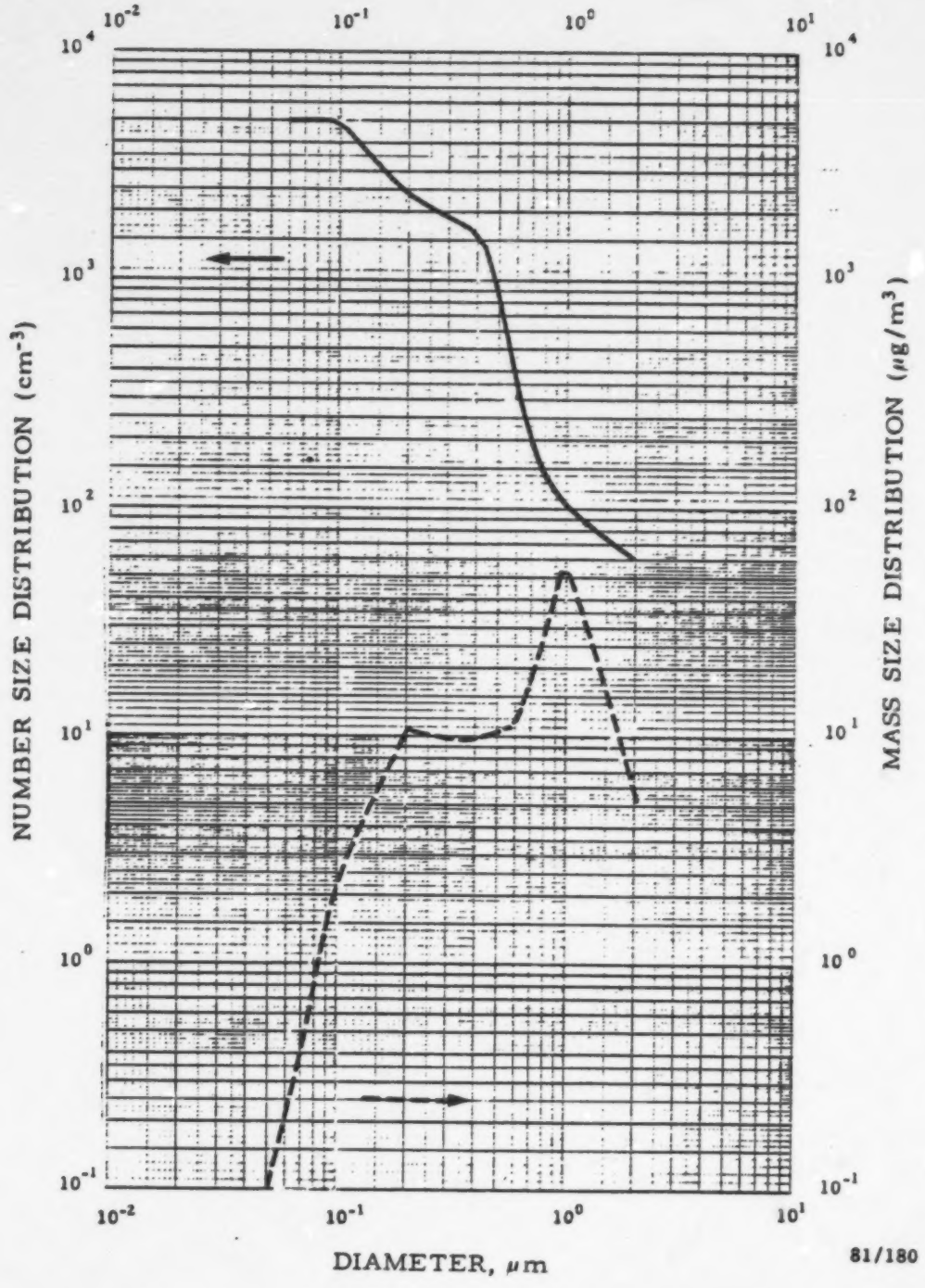

Figure A-11. Aerosol size distribution of ammonium sulfate aerosol with 1.5% methylene blue.

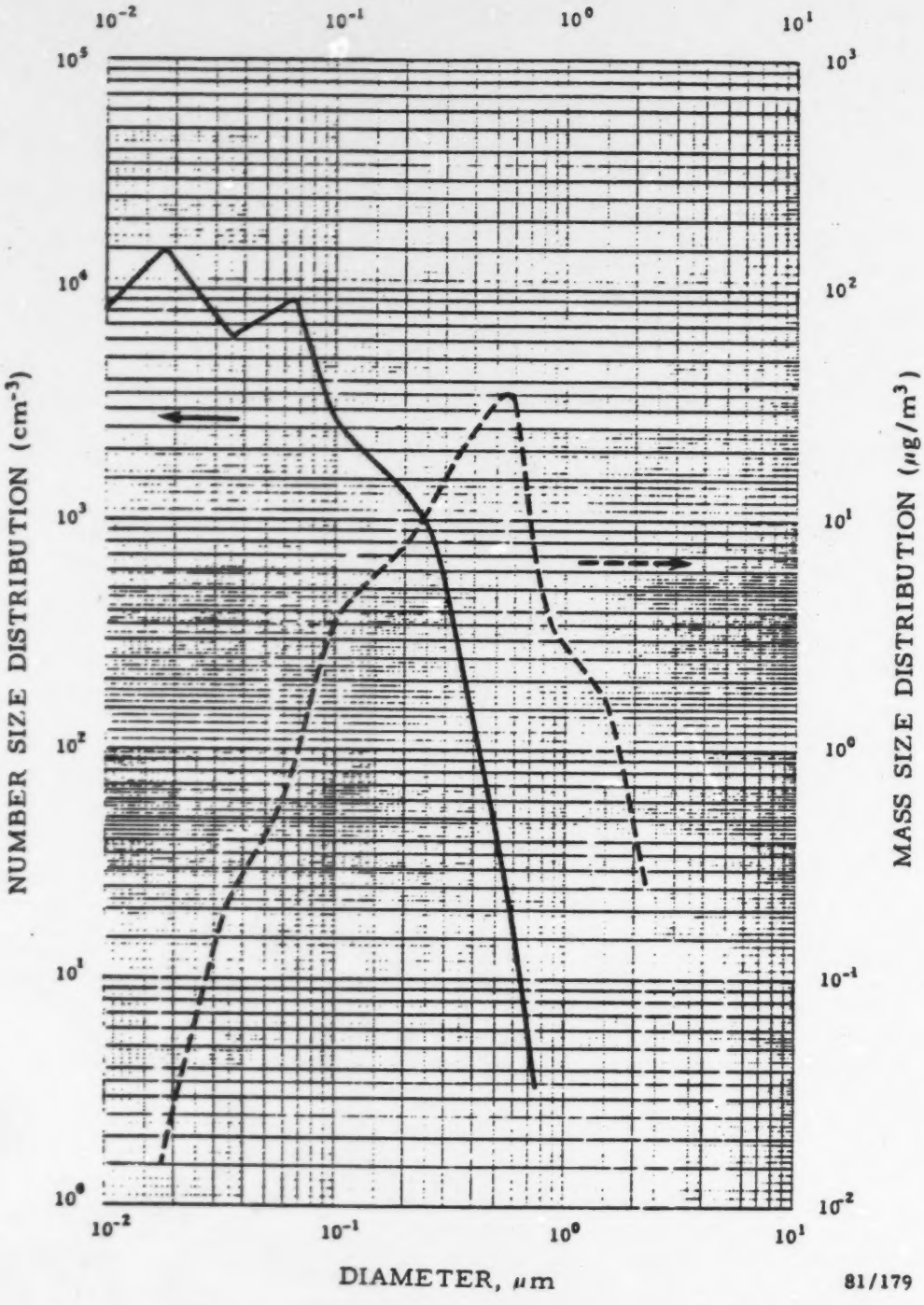

Figure A-12. Aerosol size distribution of ammonium sulfate aerosol with 4% methylene blue.

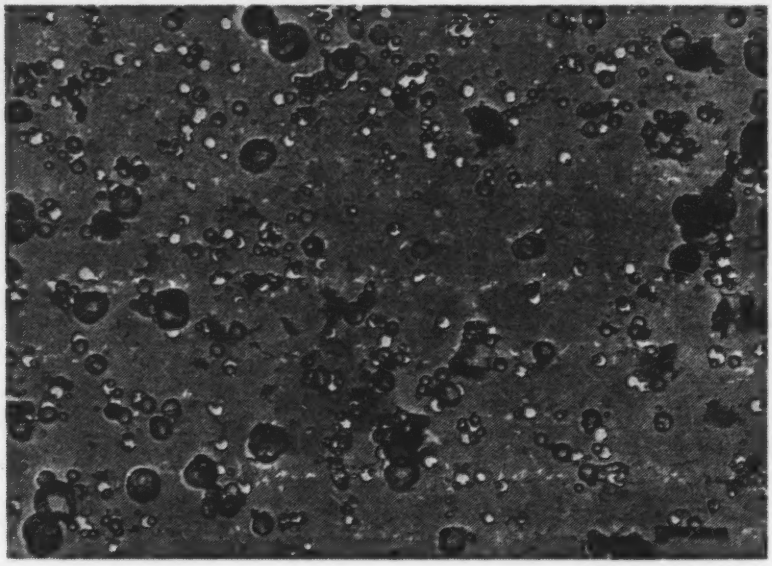

Figure A-13. Microphotograph of ammonium sulfate aerosol with 5% methylene blue (10,750X).

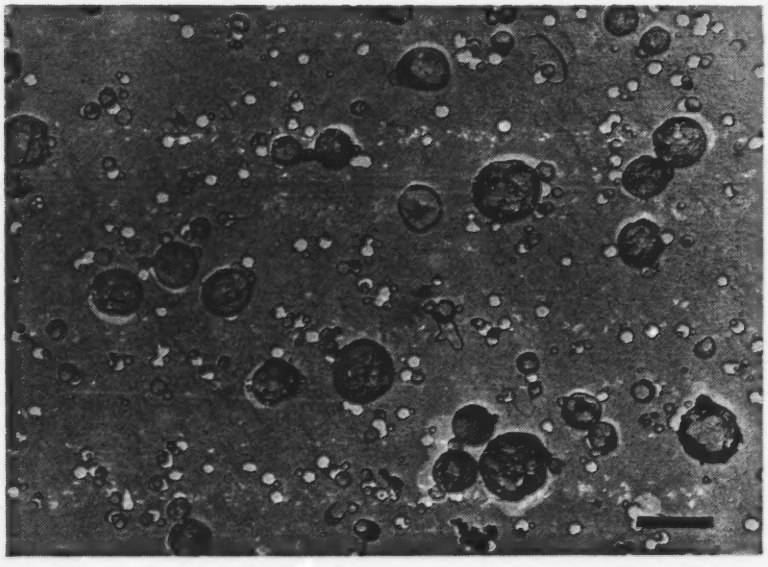

81-175

Figure A-14. Microphotograph of ammonium sulfate aerosol with 10% methylene blue (10,750X).

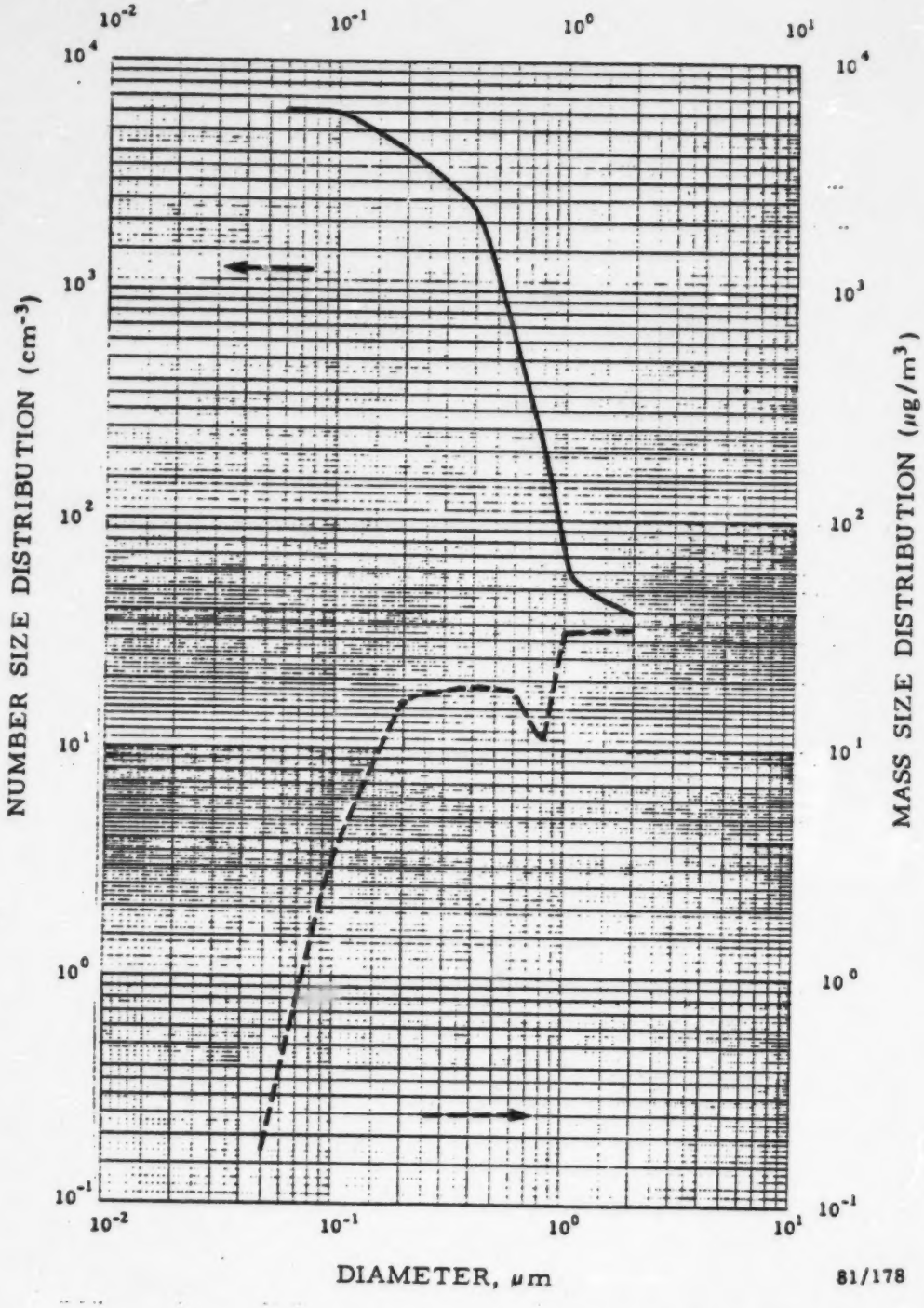

Figure A-15. Aerosol size distribution of ammonium sulfate aerosol with 5% methylene blue.

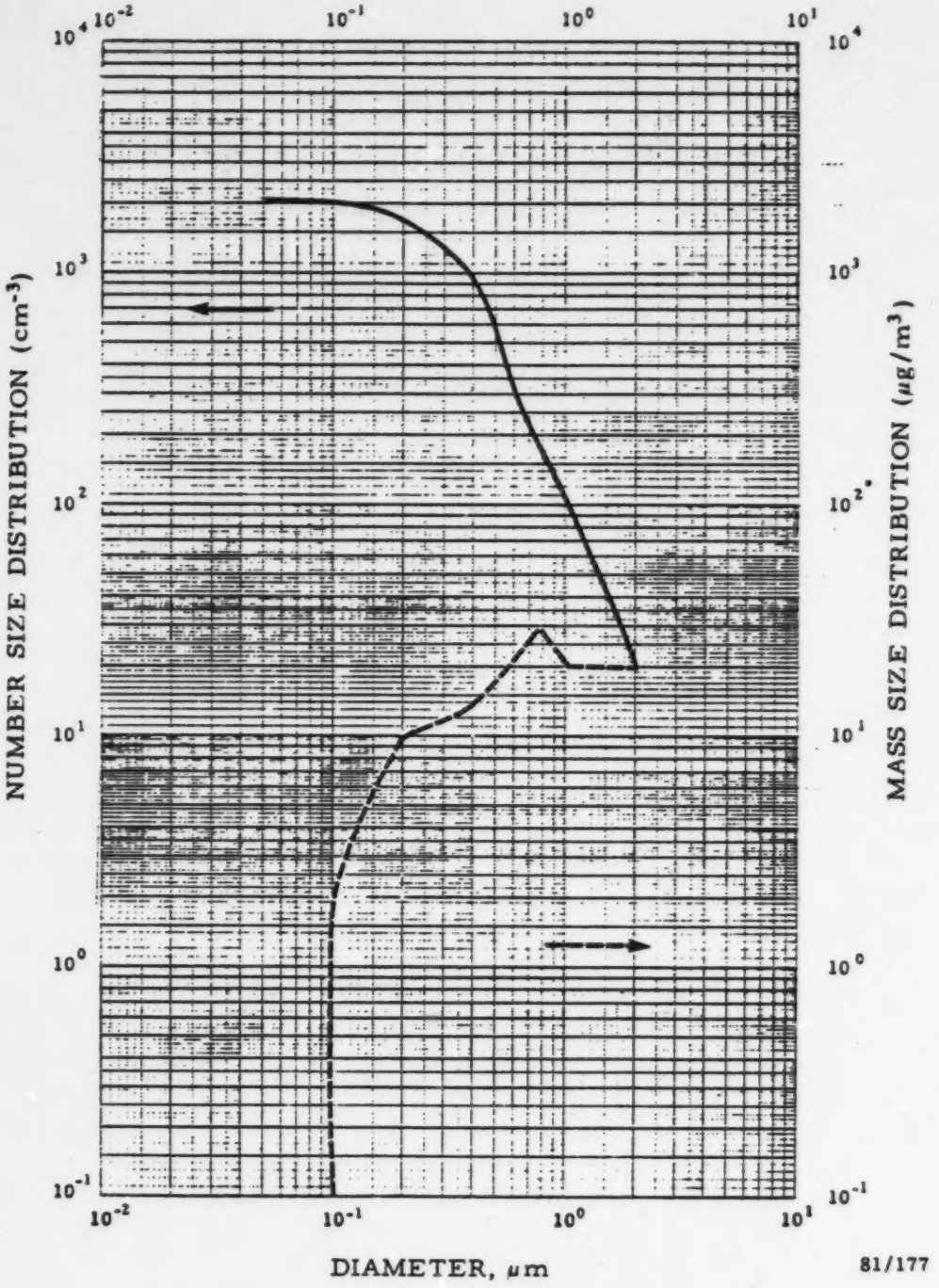

Figure A-16. Aerosol size distribution of ammonium sulfate aerosol with 10% methylene blue.

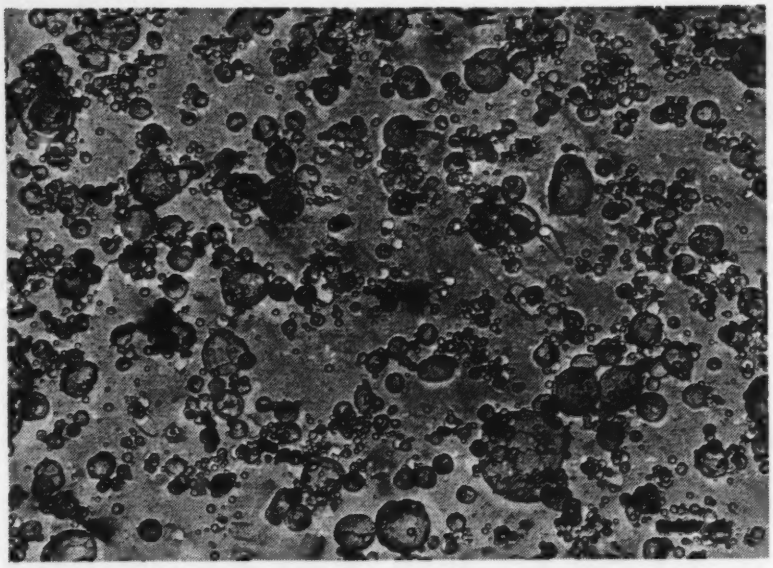

Figure A-17. Microphotograph of ammonium sulfate aerosol with 20% methylene blue (10,750X).

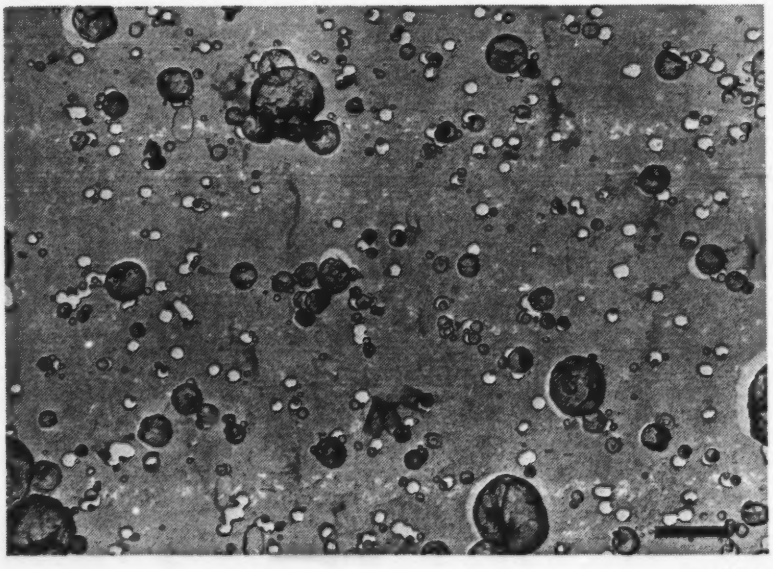

81-176

Figure A-18. Microphotograph of ammonium sulfate aerosol with 40% methylene blue (10,750X).

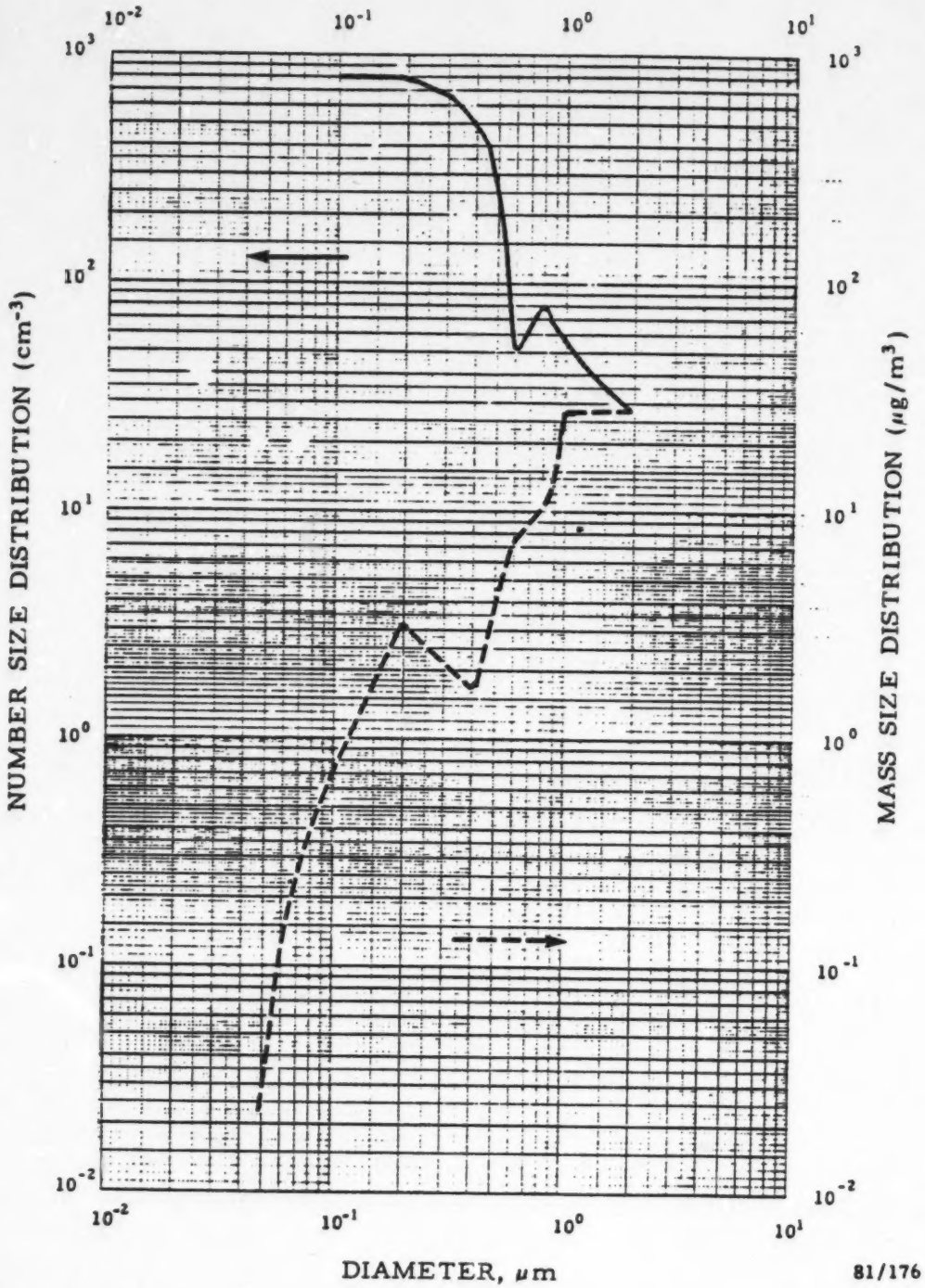

Figure A-19. Aerosol size distribution of ammonium sulfate aerosol with 20% methylene blue.

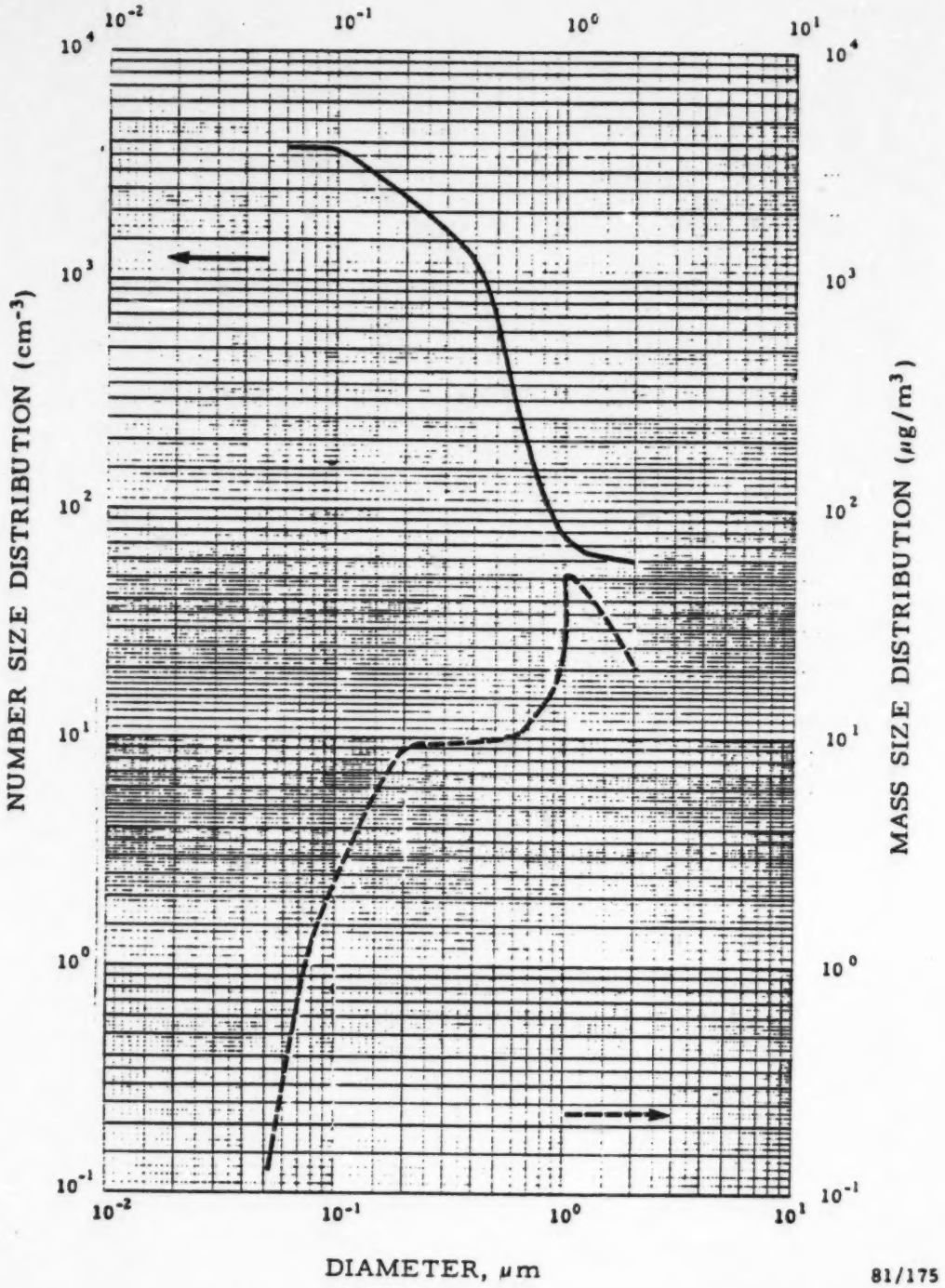

Figure A-20. Aerosol size distribution of ammonium sulfate aerosol with 40% methylene blue.

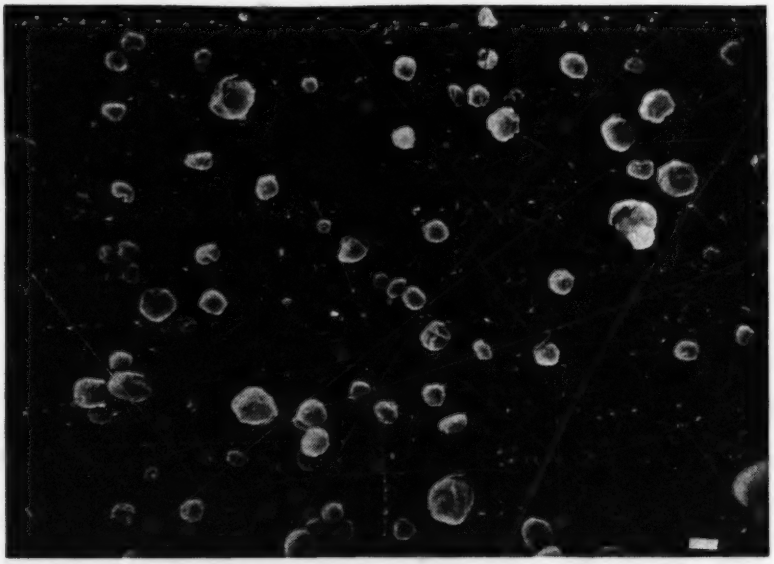

81-177

Figure A-21. Microphotograph of pure methylene blue aerosol (4000X).

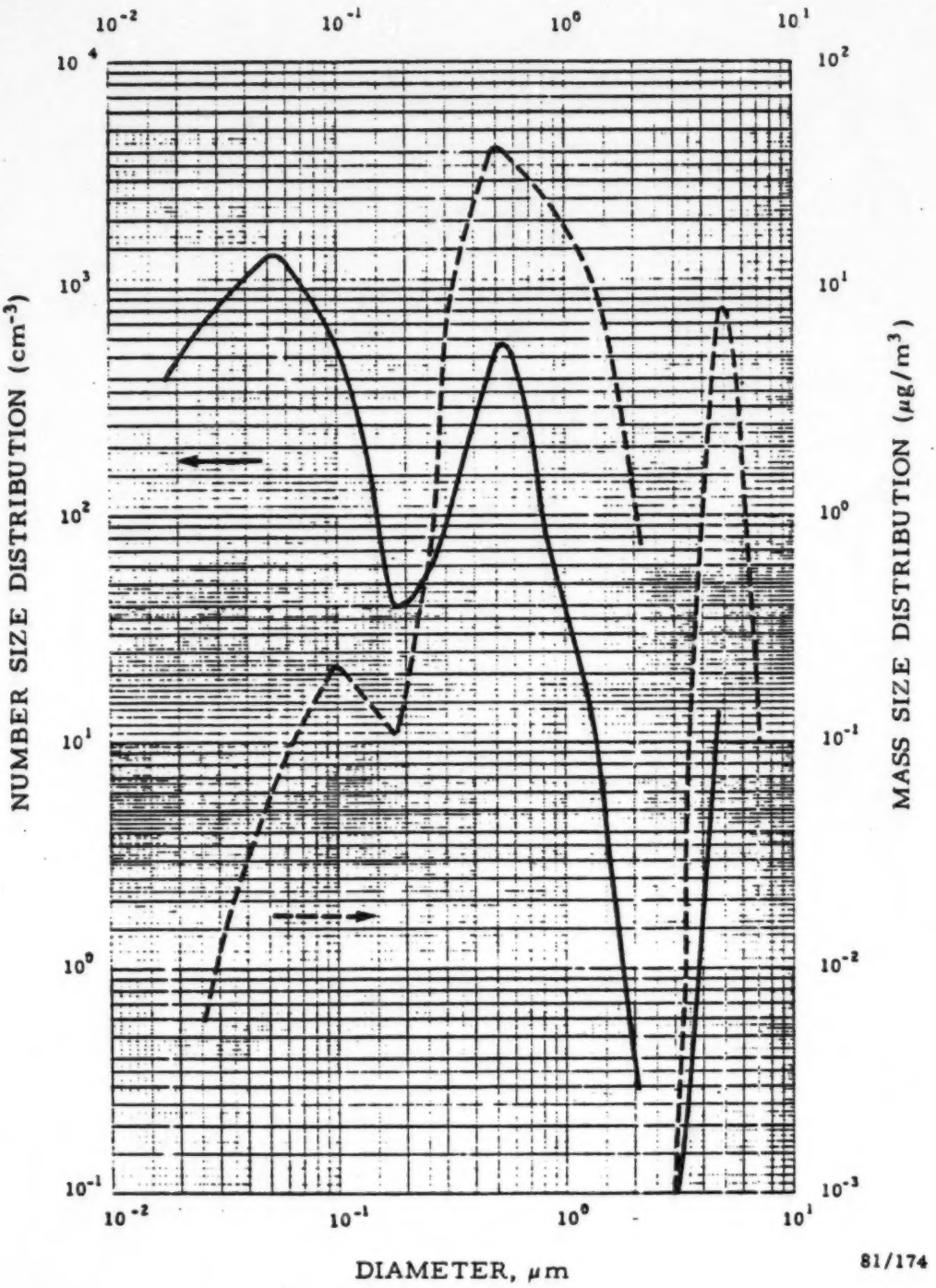

Figure A-22. Aerosol size distribution of pure methylene blue aerosol.